Prepared Under the Auspices of the U.S. Agency For International Development

Preliminary Earthquake Hazard Map of Afghanistan

By Oliver S. Boyd, Charles S. Mueller, and Kenneth S. Rukstales

Open-File Report 2007–1137

This report is USGS Afghanistan Project Product No. 156

U.S. Department of the Interior
U.S. Geological Survey

U.S. Department of the Interior
DIRK KEMPTHORNE, Secretary

U.S. Geological Survey
Mark D. Myers, Director

U.S. Geological Survey, Reston, Virginia 2007

For product and ordering information:
World Wide Web: http://www.usgs.gov/pubprod
Telephone: 1-888-ASK-USGS

For more information on the USGS—the Federal source for science about the Earth,
its natural and living resources, natural hazards, and the environment:
World Wide Web: http://www.usgs.gov
Telephone: 1-888-ASK-USGS

Any use of trade, product, or firm names is for descriptive purposes only and does not imply endorsement by the U.S. Government.

Although this report is in the public domain, permission must be secured from the individual copyright owners to reproduce any copyrighted material contained within this report.

Suggested citation:
Boyd, O.S., Mueller, C.S., and Rukstales, K.S., Preliminary probabilistic seismic hazard map for Afghanistan: U.S. Geological Survey Open-File Report 2007-1137.

Contents

Executive Summary 1
Introduction 2
Historical Earthquakes 3
Earthquake Sources 3
    Faults 3
        Chaman Fault 5
        Hari Rud Fault 6
        Central Badakhshan Fault 6
        Darvaz Fault 6
    Instrumental Seismicity 7
Earthquake Ground-motion Relations 7
    Shallow Earthquakes 8
    Deeper Earthquakes 8
Earthquake Hazard 11
    Hazard Curves 12
    Hazard Maps 12
Conclusions 19
Acknowledgments 19
References Cited 19
Glossary 21
Appendix: Primer on Probabilistic Seismic-hazard Analysis 23
    Introduction 23
    Earthquake Sources 23
    Earthquake Rates 23
    Earthquake Ground Motions 23
    Earthquake Intensity and Damage 23

Figures

1. Map of Afghanistan showing the locations of modeled fault sources 6
2. Locations of earthquakes since 1964 from the declustered catalog 8
3. Maps of modeled earthquake rates derived from smoothed seismicity showing the number of M6.0 earthquakes occurring per 10,000 km2 per 10,000 years 9
4. Maps showing the number of M6.0 earthquakes occurring per 10,000 km2 per 10,000 years between 0 and 50-km depth and the effect of various smoothing parameters 10
5. Median ground motions from selected ground-motion relations at three magnitudes for (A, B, C) Peak Ground Acceleration (PGA); (D, E, F) 0.2-second Spectral Acceleration (SA); and (G, H, I) 1.0-second SA 11
6. Hazard curves for Kabul (A, B, C), Mazar-e Sharif (D, E, F), Herat (G, H, I), and Kandahar (J, K, L) for PGA (A, D, G, J), 0.2-second SA (B, E, H, K), and 1.0-second SA (C, F, I, L) 13

7. Ground motions for fault sources for PGA (A, B), 0.2-second SA (C, D), and 1.0-second SA (E, F) at 2-percent (A, C, E) and 10-percent (B, D, F) probability of exceedance in 50 years. 14
8. Ground motions for smoothed seismicity between 0- and 50-km depth for PGA (A, B), 0.2-second SA (C, D), and 1.0-second SA (E, F) at 2-percent (A, C, E) and 10-percent (B, D, F) probability of exceedance in 50 years. 15
9. Ground motions for smoothed seismicity between 50- and 100-km depth for PGA (A, B), 0.2-second SA (C, D), and 1.0-second SA (E, F) at 2-percent (A, C, E) and 10-percent (B, D, F) probability of exceedance in 50 years. 16
10. Ground motions for smoothed seismicity between 100- and 250-km depth for PGA (A, B), 0.2-second SA (C, D), and 1.0-second SA (E, F) at 2-percent (A, C, E) and 10-percent (B, D, F) probability of exceedance in 50 years. 17
11. Ground motions for all modeled sources for PGA (A, B), 0.2-second SA (C, D), and 1.0-second SA (E, F) at 2-percent (A, C, E) and 10-percent (B, D, F) probability of exceedance in 50 years. 18

Tables

1. Selected significant earthquakes of Afghanistan 4
2. Probabilistic ground motions for selected cities 12
A1. Seismic Intensity scale with relation to ground motion 25

Plates

1. Earthquake-hazard map for Afghanistan. Modified Mercalli Intensity with a 2-percent probability of exceedance in 50 years
2. Earthquake-hazard maps for Afghanistan and hazard curves for Kabul, Herat, Kandahar, and Mazar-e Sharif

Preliminary Earthquake Hazard Map of Afghanistan

By Oliver S. Boyd, Charles S. Mueller, and Kenneth S. Rukstales

Executive Summary

The history of destructive earthquakes in Afghanistan spans more than four thousand years. Earthquakes have killed more than 7,000 Afghans in the last 10 years, including the Nahrin earthquake in May 1998 that killed an estimated 4,000 people. We expect that future large earthquakes, driven by ongoing active geologic processes in the region, will occur close to population centers and lifelines, with a consequent risk for greater casualties and damage. The seismic hazard must be considered in the siting, construction, and restoration of communities and facilities in Afghanistan.

Large earthquakes can devastate unreinforced brick and stone buildings and trigger large landslides in mountainous terrain. In 2005, the M7.6 Kashmir earthquake in Pakistan killed more than 85,000 people, injured more than 69,000, and destroyed entire towns and villages; reconstruction efforts are ongoing as we write this report. This earthquake serves as a cautionary analog for what could happen in Afghanistan in terms of magnitude, strong ground shaking, damage to structures, and landslides. Improved construction standards and techniques, guided by scientific estimates of the seismic hazard, could significantly reduce the loss of life and property.

In seismic-hazard analysis we apply knowledge of the historical earthquake record and the current tectonic environment to predict the strength of ground shaking in future earthquakes. The model that we use to evaluate hazard is composed of two elements: a source model that describes the locations, magnitudes, and rates of earthquakes, and a ground-motion model that gives the expected shaking and its variability for each earthquake. Considering a single site and a single earthquake, we can compute how often a particular ground-motion value will be exceeded. The functional relationship between exceedance rate and ground motion is a hazard curve, the fundamental result of a seismic-hazard analysis. We next consider all the earthquakes in the model, analyzing the magnitude, rate, and distance for each one and summing the exceedance rates to build up a hazard curve for the site. To make a hazard map, we do this analysis for thousands of sites covering the map area (about 35,000 sites for Afghanistan). A realistic hazard analysis involves many other details; for further information see the body and Appendix of this report.

In any seismic-hazard assessment we must recognize and account for significant model and parameter uncertainties. Seismology is a young science, and for data, seismologists must rely on limited observations and measurements of rare and unpredictable events. The century-long history of direct observation and measurement in seismology is much shorter than the recurrence times of many of the earthquakes in the model (as long as ~10,000–100,000 years). The recurrence times or fault-slip rates required in hazard models can be estimated from longer term geologic or paleoseismic data but are often highly uncertain. Large-amplitude ground motions close to faults are strongly influenced by the details of faulting and seismic-wave propagation and are highly variable, even for the same magnitude and earthquake-to-site distance. To estimate part of the hazard in Afghanistan, we rely heavily on the catalog of earthquakes recorded by global seismic networks during the past few decades, but virtually no local data exist to guide estimates of faulting or ground-shaking parameters. Fortunately, the hazard methodology incorporates parameter and modeling variability in a natural way and yields useful results even in the presence of large uncertainties.

The analysis presented here for Afghanistan is based on the same approach that is used to make the seismic hazard maps for the United States. In the United States, these maps underpin the seismic-design elements of the International Building Code and other structural-design standards. Strong ground shaking is traditionally specified by the peak horizontal acceleration of the ground expressed in units of the gravitational acceleration, g. Structural engineers sometimes prefer a so-called “spectral” motion, the response of a damped pendulum with a specific natural period (say, 1.0-second or 0.2-second period with 5 percent damping), because it can simulate the response of an idealized building. An engineer might wish to design a building to be strong enough that it has a reasonably small chance of seismic damage in the next few decades, say a 10-percent chance of damage in 50 years. The motion corresponding to this level of risk can be computed directly from the hazard curve and used in the seismic design of the building. Thus, results of a seismic hazard assessment are traditionally presented as maps of ground motion or spectral motion with a given probability of exceedance in a given time period: peak ground acceleration with a 10-percent probability of exceedance in 50 years, for example. In this report, we present maps of peak ground acceleration, 0.2-second spectral acceleration, and 1.0-second spectral acceleration, each for 2-percent and 10-percent probability of exceedance in 50 years, and corresponding hazard curves for several cities in Afghanistan.

Parts of Afghanistan lie within a relatively stable, southward-projecting promontory of the Eurasian tectonic plate, but the country is surrounded on the east, south, and west by active plate boundaries that are associated with deformation, faults, and earthquakes. The greatest hazard is in the east, where the Indian plate moves northward with

respect to Eurasia at a rate of about 4 cm/yr. A broad zone of deformation along the plate boundary lies partly within eastern Afghanistan, trending southwestward from the Hindu Kush in northeast Afghanistan, through Kabul, and along the Afghanistan-Pakistan border. This zone is characterized by abundant earthquakes and major faults. In size and slip rate, the Chaman and Central Badakhshan faults of eastern Afghanistan are comparable to other great crustal faults of the world like the San Andreas and North Anatolia faults, and the distance between Kabul and the Chaman fault is comparable to the distance between Los Angeles and the San Andreas. The Hindu Kush is one of the rare continental regions on Earth where earthquakes as deep as 200 km occur (associated with subduction of the Indian plate beneath Eurasia) and cause damage. West of Afghanistan, the Arabian plate moves northward relative to Eurasia at about 3 cm/yr. The main plate boundary trends northwestward through the Zagros region of southwestern Iran. Although Iran is laced with major faults, and earthquakes are common, the deformation for the most part does not cross the border, leaving western Afghanistan relatively quiescent seismically.

Our source model for Afghanistan uses data from the global catalog of earthquakes with magnitudes equal to or greater than about 4.5 since 1964. We also include four specific faults in the model, using slip rates estimated from geologic data. Lacking local ground-motion-prediction relations, we apply estimates from analogous active tectonic regions in western North America, Europe, and the Middle East for shallow sources and estimates from global subduction earthquake data sets for deeper sources.

Our analysis shows that seismic hazard is high in northeastern Afghanistan and much lower in the western half of the country. Hazard levels in Kabul, with contributions from both the regional seismicity and the nearby Chaman fault, are roughly similar to those found in some seismically active parts of the intermountain West in the United States. Hazard increases northeast of Kabul through the Hindu Kush, due in part to the increased seismicity there, and near the traces of the Central Badakhshan and Darvaz faults, hazard levels approach those found in some seismically active parts of California.

These preliminary seismic-hazard maps are based on the currently available data and our best scientific judgments based on these data. Owing to the limited number of field investigations of potentially active faults and limited local earthquake monitoring, modeling and parameter uncertainties are significant. The maps will change in the future as we learn more about the earthquake history and potential of the region.

Introduction

Earthquakes represent a serious threat to the people and institutions of Afghanistan. As part of a United States Agency for International Development (USAID) effort to assess the resource potential and seismic hazards of Afghanistan, the Seismic Hazard Mapping group of the United States Geological Survey (USGS) has prepared a series of probabilistic seismic hazard maps that help quantify the expected frequency and strength of ground shaking nationwide. To construct the maps, we do a complete hazard analysis for each of ~35,000 sites in the study area. We use a probabilistic methodology that accounts for all potential seismic sources and their rates of earthquake activity, and we incorporate modeling uncertainty by using logic trees for source and ground-motion parameters. See the Appendix for an explanation of probabilistic seismic hazard analysis and discussion of seismic risk.

Afghanistan occupies a southward-projecting, relatively stable promontory of the Eurasian tectonic plate (Ambraseys and Bilham, 2003; Wheeler and others, 2005). Active plate boundaries, however, surround Afghanistan on the west, south, and east. To the west, the Arabian plate moves northward relative to Eurasia at about 3 cm/yr. The active plate boundary trends northwestward through the Zagros region of southwestern Iran. Deformation is accommodated throughout the territory of Iran; major structures include several north-south-trending, right-lateral strike-slip fault systems in the east and, farther to the north, a series of east-west-trending reverse- and strike-slip faults. This deformation apparently does not cross the border into relatively stable western Afghanistan. In the east, the Indian plate moves northward relative to Eurasia at a rate of about 4 cm/yr. A broad, transpressional plate-boundary zone extends into eastern Afghanistan, trending southwestward from the Hindu Kush in northeast Afghanistan, through Kabul, and along the Afghanistan-Pakistan border. Deformation here is expressed as a belt of major, north-northeast-trending, left-lateral strike-slip faults and abundant seismicity. The seismicity intensifies farther to the northeast and includes a prominent zone of deep earthquakes associated with northward subduction of the Indian plate beneath Eurasia that extends beneath the Hindu Kush and Pamirs Mountains.

Production of the seismic hazard maps is challenging because the geological and seismological data required to produce a seismic hazard model are limited. The data that are available for this project include historical seismicity and poorly constrained slip rates on only a few of the many active faults in the country. Much of the hazard is derived from a new catalog of historical earthquakes: from 1964 to the present, with magnitude equal to or greater than about 4.5, and with depth between 0 and 250 kilometers. We also include four specific faults in the model: the Chaman fault with an assigned slip rate of 10 mm/yr, the Central Badakhshan fault with an assigned slip rate of 12 mm/yr, the Darvaz fault with an assigned slip rate of 7 mm/yr, and the Hari Rud fault with an assigned slip rate of 2 mm/yr. For these faults and for shallow seismicity less than 50 km deep, we incorporate published ground-motion estimates from tectonically active regions of western North America, Europe, and the Middle East. Ground-motion estimates for deeper seismicity are derived from data in subduction environments. We apply estimates derived for tectonic regions where subduction is the main tectonic process for intermediate-depth seismicity between 50- and 250-km depth.

Within the framework of these limitations, we have developed a preliminary probabilistic seismic-hazard assessment of Afghanistan, the type of analysis that underpins the seismic components of modern building codes in the United States. The assessment includes maps of estimated peak ground-acceleration (PGA), 0.2-second spectral acceleration (SA), and 1.0-second SA, with return periods of about 500 years (equal to a 10-percent probability in 50 years) and 2,500 years (equal to a 2-percent probability in 50 years).

Historical Earthquakes

Although some evidence exists for earthquakes in Afghanistan as far back as 2000 B.C., Ambraseys and Bilham (2003) begin the documented seismic history in the region with Persian accounts from the eighth century A.D. Much of the historical record is incomplete and informal, but narrative accounts of shaking, damage, casualties, landslides, and other earthquake effects can be used to refine estimates of earthquake locations and magnitudes and even constrain pre instrumental rates of seismic energy release. Narrative accounts can also provide a broader context for a seismic hazard analysis, such as the one presented here, that is based on only a few decades of modern seismographic data.

For earthquakes in the pre instrumental era (before ~1900), Ambraseys and Bilham (2003) estimated locations and surface-wave magnitudes (M_s) from narrative accounts of felt area and damage intensity. For earthquakes in the early instrumental era, they critically reassessed published locations in light of similar narrative accounts and computed more than 500 new M_s values from station bulletin data. With the new catalog, they were able to analyze the entire 1,200-year-long record in the context of modern plate tectonics and seismic-hazard ideas. Ambraseys and Bilham (2003) also provided extended documentation for 47 earthquakes; we summarize these accounts in table 1 for a few significant events. It is important to note that many earthquakes in Afghanistan other than those listed in table 1 have caused damage and casualties. Due largely to inadequate construction practices in the region, relatively small earthquakes have caused fatalities. Northeastern Afghanistan is one of the rare continental regions on Earth where destructive earthquakes occur at depths of 200 km or more.

Earthquake Sources

We use two primary sources of information to estimate the hazard from future earthquakes in Afghanistan: (1) geologic data on active faults, and (2) data for earthquakes that have been recorded on seismographs. In general, these sources are in close agreement with the historical information.

Many faults in Afghanistan are thought to be active, either from spatial association with earthquakes, from their geologic expression, or, more rarely, from direct observation of surface rupture. Unfortunately, most suspect faults have not been studied and characterized in sufficient detail to allow them to be explicitly modeled in a seismic hazard assessment. Faults without sufficient information are considered to be captured by the instrumental-seismicity model. The instrumental catalog provides accurate locations, times, and magnitudes of earthquakes, especially since the 1960s when the first global seismograph networks were installed. We therefore base our analysis on the instrumental catalog for earthquakes of magnitude 4.5 and greater occurring since 1964, and the four active faults discussed herein.

Faults

Little data are available to guide models of slip rates or recurrence times for large earthquakes on individual faults in Afghanistan. Some faults are known to be active because historical accounts describe surface rupture corresponding to large earthquakes (Quittmeyer and Jacob, 1979; Yeats and others, 1979; Lawrence and others, 1992). We rely heavily on the information described by Wheeler and others (2005) and Ruleman and others (2007), who identify several faults as possibly being active. Of the potentially active faults, we include the Chaman fault, the Hari Rud fault, the Central Badakhshan fault, and the Darvaz fault as those most likely to contribute to seismic hazard and having sufficient information to be includes in a seismic-hazard analysis (fig. 1).

These faults have dimensions and surface expressions that are similar to major, continent-scale, strike-slip fault systems worldwide, including better-studied faults such as the San Andreas, the Anatolian, and the Denali fault systems. Each of these is capable of producing earthquakes in the moment-magnitude range from upper 7 to near 8. For example, the 1857 Fort Tejon earthquake on the southern San Andreas fault probably had an M_w 7.9 (Townley, 1939; Sieh, 1978), and the 1906 San Francisco earthquake had an M_w ~7.8 (Lawson, 1908; Ellsworth, 1990). Historical earthquakes in the moment-magnitude 6.9 to 8.0 range have ruptured large parts of the Anatolian fault system in Turkey, and in 2002, an M_w 7.9 earthquake produced 347 km of surface rupture on the Denali and associated faults in Alaska (Haeussler and others, 2004). Given these analogs with respect to fault length, slip rate, and surface expression, we consider it possible that the major strike-slip faults in Afghanistan are capable of producing similar large-magnitude earthquakes.

We follow the methodology that is used for the USGS national seismic hazard maps of the United States, and we consider two types of earthquake-recurrence behavior: a characteristic model and a Gutenberg-Richter (or truncated exponential) model. The characteristic model applies to a fault that repeatedly produces large-magnitude earthquakes in a narrow magnitude range with few smaller earthquakes. The Gutenberg-Richter model applies to a fault that produces a range of earthquake sizes. A truncated exponential frequency-magnitude distribution is recognized to apply to most regional earthquake

Table 1. Selected significant earthquakes of Afghanistan.[1]

Date, A.D.	Estimated M_s	Estimated Lat.	Estimated Long.	Description
819	7.4	36.4°N	65.4°E	The earliest well-documented earthquake occurred in northern Afghanistan, ~150 km west of Mazar-e Sharif, in A.D. 819. Heavy casualties and damage were reported in several villages many tens of kilometers apart.
849	5.3	34.3°N	62.2°E	These earthquakes caused heavy damage and some casualties in Herat, noteworthy since our seismic hazard analysis finds relatively lower hazard near Herat.
1102	5.3	34.4°N	62.2°E	
1364	5.8	34.9°N	61.7°E	
1505	7.3	34.5°N	69.1°E	This earthquake caused damage in Kabul, and heavy casualties and damage in Paghman (~20 km west of Kabul) and nearby villages. Accounts suggest that the earthquake occurred on the Paghman fault, the northern extension of the Chaman fault between Kabul and the junction of the Hari Rud and Central Badakhshan faults, with at least 40 km of surface rupture and vertical offsets up to 3 m. A possible strike-slip component is undocumented.
22 Jan 1832	7.4	36.5°N	71.0°E	Centered in the Badakhshan district of northeast Afghanistan, this large earthquake reportedly destroyed many villages and killed thousands of people. The shock triggered numerous landslides and rockfalls and was strongly felt in Kabul and Lahore. Based on its location in the Hindu Kush of northeast Afghanistan and large felt area (radius ~450 km), this earthquake has been interpreted as a subcrustal event (depth ~180 km) by Russian researchers.
19 Feb 1942	7.5	35.0°N	71.0°E	British soldiers and their dependents stationed in the region provided detailed accounts of this large earthquake. Damage patterns suggest that it was centered near Jalalabad in northeast Afghanistan and was possibly associated with oblique thrust faulting along the southern reach of the Konar fault system.
18 Oct 1874	7.0	35.1°N	69.2°E	This earthquake caused heavy damage and casualties in villages ~70 km north of Kabul (also possibly in Kabul itself).
20 Dec 1892	6.5	30.9°N	66.5°E	Located near the Pakistan border, ~90 km northwest of Quetta, this earthquake caused surface rupture (of undocumented length) on the Chaman fault.
7 July 1909	7.5	36.5°N	70.5°E	Ambraseys and Bilham (2003) interpret this as a double earthquake: a shallow ~M_s7.5 event followed one minute later by a deep ~M_s7.5 event. This interpretation is based on the 700-km radius of perceptibility (suggesting a deep earthquake), and patterns of localized, strong damage in the Badakhshan region of northeast Afghanistan (suggesting a shallow earthquake).
1 Jan 1911	7.1	36.5°N	66.5°E	This earthquake was widely felt in northern Afghanistan and adjacent Tajikistan. Damage and casualties were centered in the mountains north of Kabul. The mainshock was followed by a M_s6.5 aftershock 4 hours later.
30 May 1935	7.7	28.9°N	66.4°E	This major earthquake was centered across the southeastern border of Afghanistan, near Quetta, Pakistan. Damage and casualties were concentrated in a narrow zone (~160x25 km) extending southward from Quetta. Houses in the region were built chiefly of non resistant mud brick, and Ambraseys and Bilham (2003) estimate that all the villages in the damage zone were destroyed with 70 percent of the population dead or injured. Of ~35,000 total fatalities, ~26,000 occurred in Quetta, which was almost totally destroyed. Some researchers associate this earthquake with the Ghazaband fault zone, part of a system of north-south-trending faults that accommodates left-lateral shearing along the Eurasia-Indian plate boundary midway between Quetta and the Afghanistan-Pakistan border.

Table 1. Selected significant earthquakes of Afghanistan (cont'd).

Date, A.D.	Estimated M_s	Estimated Lat.	Estimated Long.	Description
9 June 1956	7.4	35.1°N	67.5°E	Centered ~160 km northwest of Kabul in a sparsely populated region of northern Afghanistan, this large earthquake destroyed several mountain villages.
3 Oct 1975	6.8	30.2°N	66.3°E	This earthquake occurred in a sparsely populated region of southeast Afghanistan. Apparent co-seismic slip on the Chaman fault, ~4 cm of left-lateral displacement with a minor component of up-to-the-west dip slip, extended for a distance of ~5 km. The mainshock was followed 12 hours later by a M_s6.5 aftershock.
16 Dec 1982	6.5	36.1°N	69.0°E	Centered in the mountains ~170 km north of Kabul, this earthquake was felt over a radius of 500 km, destroyed 7,000 houses, and killed 450 people.
4 Feb 1998	5.9	37.1°N	70.1°E	This earthquake was located in the mountains ~300 km north of Kabul. Shaking triggered many destructive landslides. Estimated losses included 2,300 people killed and 8,000 homeless.
30 May 1998	6.5	37.1°N	70.1°E	Located near the site of 4 Feb 1998 shock, this earthquake killed ~4,000 people.
3 Mar 2002	7.4	36.5°N	70.48°E	Centered in the Hindu Kush region, this is an example of a deep earthquake (~200 km depth) that caused damage and fatalities. Ambraseys and Bilham (2003) note six fatalities in Kabul and extensive damage in a few villages, but a general lack of injuries and fatalities in rural areas. USGS notes 13 fatalities in Kabul and Rostaq, and 150 people killed by a landslide.

[1]The information in this table is derived from Ambraseys and Bilham (2003). See tables 1 and 2 and the Electronic Supplement therein for additional information.

catalogs, but it can also be used to model behavior on specific faults. It is defined such that the cumulative number of earthquakes above magnitude *M* per unit time is equal to 10*a-bM* where *a* and *b* are constants. The *b-value* is often close to 1, meaning that magnitude M-1 earthquakes occur about 10 times more often than magnitude M. For a fault, the *a-value, the earthquake activity rate*, can be chosen such that the seismic moment released in earthquakes is equal to the moment budget based on the geometry of the fault and the slip rate.

We apply a 66-percent weighting factor to the characteristic-earthquake behavior and a 33-percent weighting factor to the Gutenberg-Richter behavior. We use an M_w of 7.9 for the characteristic earthquake and apply a standard deviation of ±0.2 magnitude units to account for uncertainty. We exponentially distribute earthquakes in the moment-magnitude range of 7.3–7.9 for the Gutenberg-Richter behavior and allow the instrumental-seismicity part of the model (below) to account for hazard from earthquakes in the moment-magnitude range of 5.0, a traditional lower threshold for damage, to 7.3. A *b*-value of 1.0, used for both the Gutenberg-Richter behavior of specific faults and the instrumental-seismicity model, was determined from analysis of instrumental seismicity. There are almost certainly other active faults in Afghanistan that are capable of producing large earthquakes. Lacking sufficient information to explicitly include them in our hazard model, however, we must rely on the instrumental-seismicity part of the model (described in the section on "Instrumental Seismicity") to capture the hazard associated with these structures.

Chaman Fault

The Chaman fault system is more than 1,000 km long, extending from the Hindu Kush region in northeastern Afghanistan south-southwestward through eastern Afghanistan into western Pakistan. Several large historical earthquakes have produced surface rupture on the fault in Afghanistan. In 1505, an earthquake having an estimated magnitude of M_s 7.3 occurred near Kabul, producing about 40–60 km of surface rupture and several meters of vertical offset (Quittmeyer and Jacob, 1979; Ambraseys and Bilham, 2003). The "Paghman" fault mentioned in table 1 is part of the Chaman fault system (R. L. Wheeler, oral commun., 2007). An earthquake in 1892 occurred near 31°N., producing 60–75 cm of left-lateral movement and dropping the west side of the fault by 20–30 cm (Quittmeyer and Jacob, 1979; Lawrence and others, 1992). A moment-magnitude (M_w) 6.4 earthquake in 1975 near 30°N. produced 5 km of surface rupture, 4 cm of left-lateral offset, and a small amount of east-side-down slip (Yeats and others, 1979).

Based on studies of aerial photographs and Quaternary geomorphology, Tapponier and others (1981) and Wellman (1965) estimated slip rates on the Chaman fault system to be between 2 and 20 mm/yr. Lawrence and others (1992) suggested that the slip rate on the southern end of the fault may be higher where it enters western Pakistan. Despite the large uncertainty in the estimated slip rate, the Chaman fault system poses a significant seismic hazard that needs to be

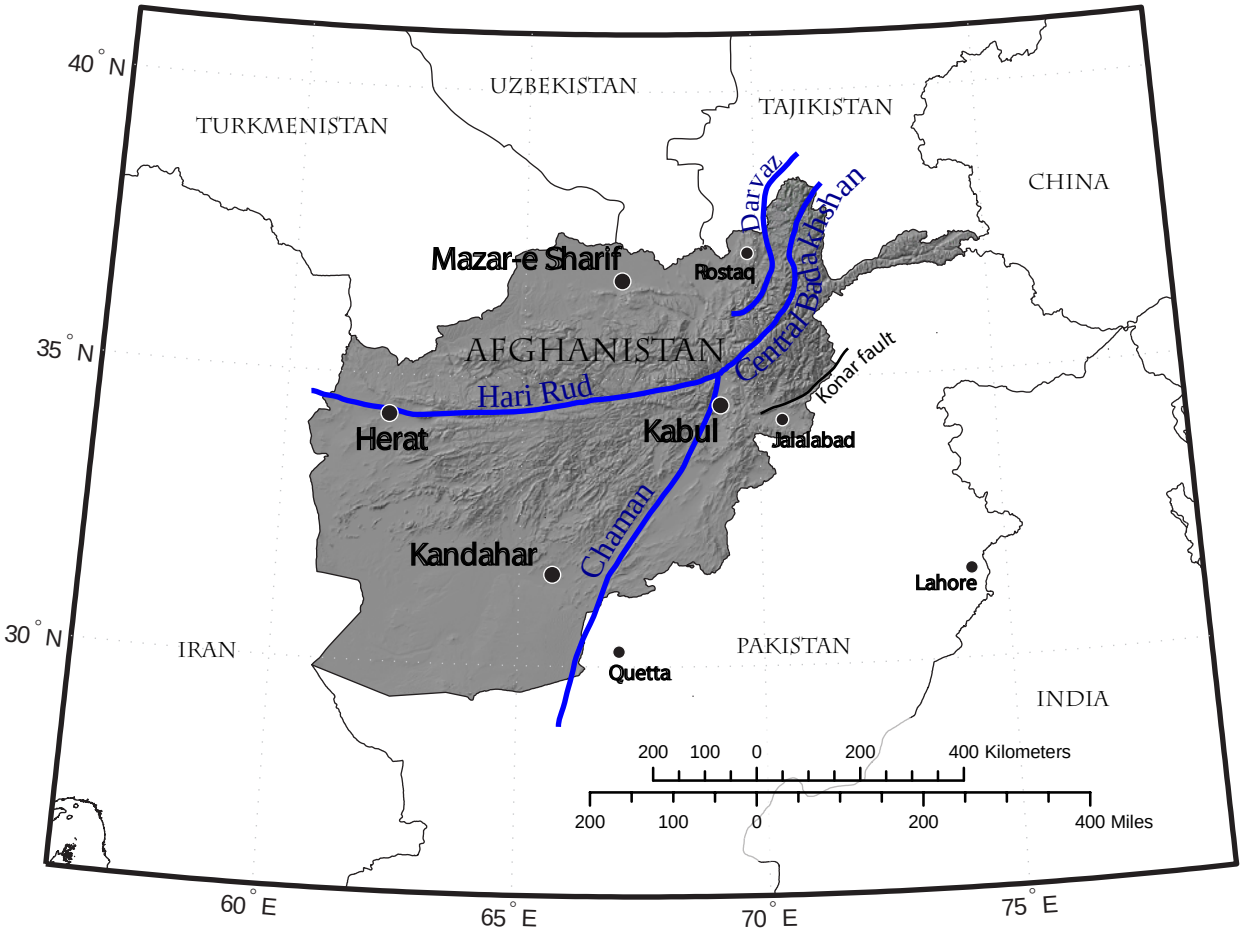

Figure 1. Map of Afghanistan showing the locations of modeled fault sources (heavy blue lines).

incorporated into our analysis. We assign a slip rate of 10 mm/yr to the Chaman fault system south of the junction with the Hari Rud fault but recognize that this value will almost certainly be revised when detailed geological field studies of the fault provide better measurements of its slip rate.

Hari Rud Fault

The 730-km-long, right-lateral Hari Rud fault extends from its intersection with the Chaman fault north of Kabul westward to the Iran border. The fault has an exceptional geomorphic expression on the landscape, due in large part to the region's arid climate and much of the fault being located in hard bedrock, but other evidence for active faulting remains controversial (Wellman, 1965; Trifonov, 1978). Sborshchikov and others (1981) report that the fault appears to have laterally offset stream channels 5 km since late Pliocene time (about 2 million years ago), yielding a long-term slip rate of about 3 mm/yr. Considering this to be an upper bound, we use a slip rate of 2 mm/yr in our model.

Central Badakhshan Fault

Wheeler and others (2005) did not find a published slip rate for the Central Badakhshan fault. Assuming that the slip rate is conserved at the junction of the Hari Rud and Chaman faults, we assign a slip rate of 12 mm/yr for the Central Badakhshan fault.

Darvaz Fault

The 380-km-long, left-lateral Darvaz fault parallels the Central Badakhshan fault in northeastern Afghanistan and, like it, extends northward into Tajikistan. The Darvaz fault is located in a region of abundant seismicity, and Trifonov (1978) reported that landforms of late Holocene, Holocene, and late Pleistocene age are laterally offset 20, 120, and 300 m, respectively. Wheeler and others (2005) estimated very approximate ages of 3 ka, 10 ka, and 130 ka for these features to infer slip rates of 7, 12, and 2 mm/yr, respectively. For our model, we use a median slip rate of 7 mm/yr for the fault.

Instrumental Seismicity

We prefer not to use earthquake data from the pre instrumental era directly in our analysis because the locations and magnitudes of these earthquakes are highly uncertain and the record is incomplete. The locations and magnitudes of earthquakes that have been recorded by seismographs are generally more accurate than those based on historical accounts. For many decades, however, there were few seismographs in this part of the world, so even during the modern era of seismology, reliable catalogs must be based on earthquakes large enough to have been recorded on global seismograph networks. We use a catalog that contains only instrumentally recorded earthquakes with magnitude equal to or greater than about M_w 4.5 since 1964, a time when the Worldwide Standardized Seismographic Network (WWSSN) was largely deployed and data from the network were widely available. These choices are made to minimize the effects of catalog incompleteness and uncertainty while still including enough of the seismic record to represent the locations, rates, and magnitudes of future earthquakes.

Dewey and others (2006) provide an overview of the historical and instrumental seismicity in Afghanistan and the surrounding region, and Bergman (2006) describes the procedures and criteria used to construct a comprehensive catalog of instrumentally recorded earthquakes for the region. Bergman combined and analyzed information from several published sources to create a consistent summary catalog with a preferred origin time, location, and magnitude for each earthquake. He also relocated and updated the origin times of many earthquakes by using updated software and earth structure models.

In the hazard analysis, ground motions for each modeled earthquake are computed as a function of source-to-site distance and moment magnitude. In Bergman's catalog, magnitudes for most of the largest earthquakes are moment magnitudes derived from published special studies or determined by the routine global earthquake studies of Harvard University or the USGS. In the post-1960 era, magnitudes for all but the largest earthquakes are dominated by teleseismic body-wave (m_b) and surface-wave (M_s) magnitudes reported by the International Seismological Centre (ISC) or the USGS. We convert m_b and M_s to M_w using relations that account for the effects of magnitude saturation and source scaling (see, for example, Utsu, 2002; Sipkin, 2003). Bergman's catalog contains 11,900 that occurred between 1964 and 2004 above magnitude 4.

Using the time- and distance-windowing algorithm of Gardner and Knopoff (1974), we declustered the catalog to remove aftershocks and foreshocks; our hazard analysis assumes a catalog of independent earthquakes. Based on a completeness analysis of the declustered catalog, we further reduce this catalog to approximately 2,000 earthquakes that occurred between 1964 and 2004 that have an M_w of 4.5 or greater and that have a depth of 250 km or shallower (fig. 2). We subdivide the catalog into five depth ranges, 0–50 km, 50–100 km, 100–150 km, 150–200 km, and 200–250 km, and, as described in the section on "Earthquake Ground-Motion Relations", apply different ground-motion estimates for the different depth ranges to compute the hazard.

From each depth subset of the catalog, we determine earthquake rates for cells on a grid that spans the entire study area. Nodes of the grid are spaced at increments of 0.1° in latitude and longitude following the methodology of Frankel and others (1996). We assume that the earthquakes occur at a rate that follows a Gutenberg-Richter distribution with a *b*-value of 1.0 and compute the rate for each grid cell by counting earthquakes (Weichert, 1980) with M_w equal to or greater than 4.5 between 1964 and 2004. To account for uncertainty, these rates are spatially smoothed over a distance greater than the grid node spacing.

Grid nodes for the four deeper subsets between 50- and 250-km depth are smoothed with a 2-dimensional Gaussian kernel that has a correlation distance of 50 km, while grid nodes for the shallow seismicity less than 50-km depth are smoothed with a variable width ranging between 50 and 150 km (fig. 3). The smoothing width is increased until either (1) three earthquakes are located within a smoothing width or (2) the maximum smoothing width is reached. We chose the minimum number of earthquakes within a smoothing width and the maximum smoothing width to minimize bullseye-type artifacts created by isolated earthquakes and rate changes in low-seismicity regions (fig. 4).

Note that earthquakes located outside Afghanistan, particularly deep earthquakes beneath south Tajikistan, could cause significant damage in Afghanistan.

Earthquake Ground-motion Relations

We use one set of ground-motion relations for the intermediate-depth earthquakes and another set for the shallow earthquakes because the excitation of seismic energy and wave-propagation effects are different for earthquakes in different depth ranges. Both sets of relations are derived from empirical studies of ground motions from earthquakes in active tectonic regions analogous to Afghanistan. For shallow earthquakes, we use one relation based on data from Europe and the Middle East and several relations based on large, well-studied data sets from western North America. For the intermediate-depth seismicity, we use a set of relations that were derived from global data sets that contained primarily intermediate-depth earthquakes in subduction-zone tectonic settings. As in the national seismic hazard maps for the United States, the hazard is calculated for an assumed firm-rock site condition with an average shear-wave velocity in the upper 30 meters (V_s30) of 760 m/s. Ground motions for a specific site must be converted from this reference site condition to conditions appropriate for the local site.

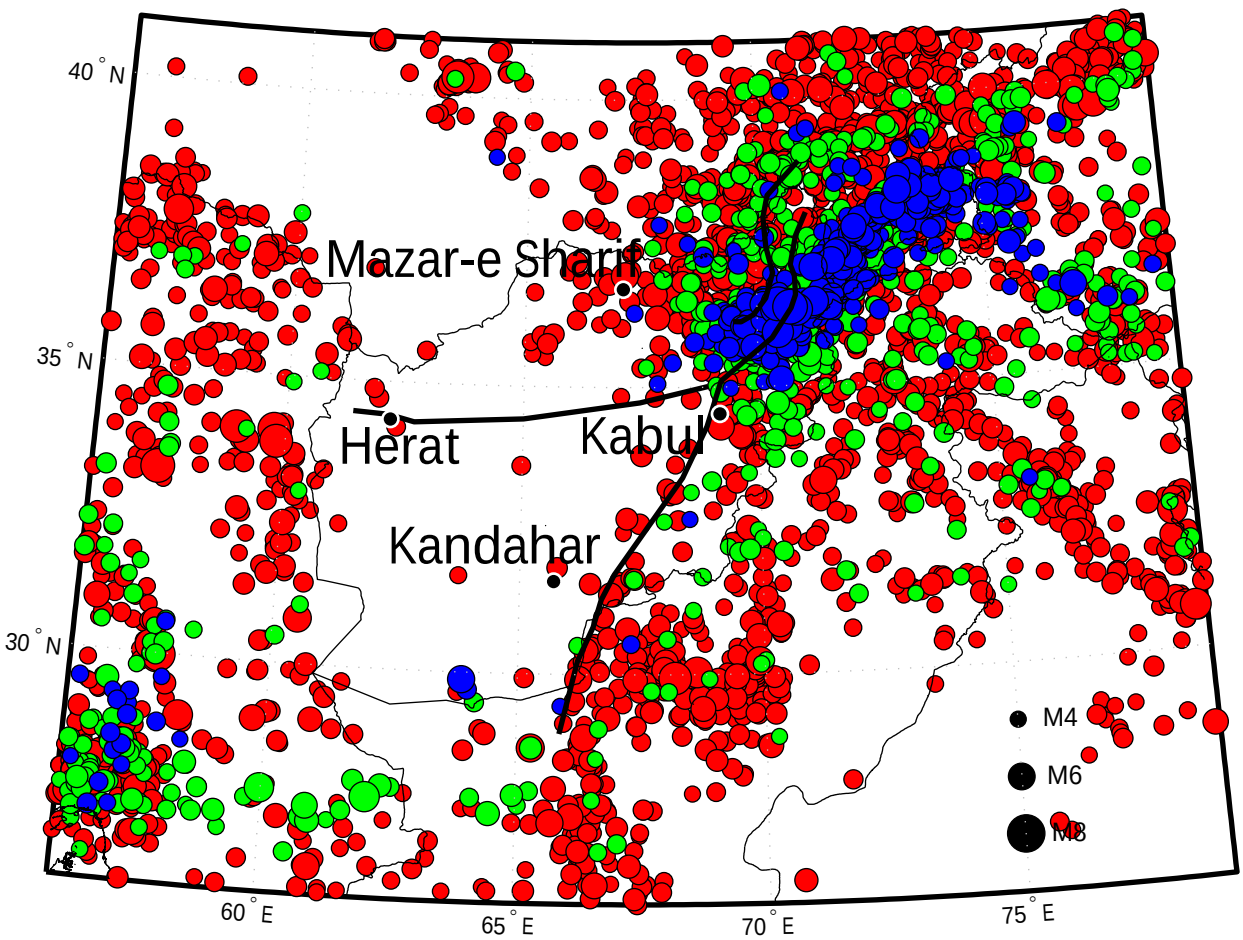

Figure 2. Locations of earthquakes since 1964 from the declustered catalog; red: 0–50 km depth, green: 50–100 km depth, and blue: 100–250 km depth.

Shallow Earthquakes

Zare and Bard (1999) developed relations for PGA for shallow earthquakes in Iran. Though arguably the most applicable relations because of the proximity to Afghanistan, we chose not to use the Zare and Bard relations because they do not predict spectral accelerations. Instead, we chose to use the relations developed by Ambraseys and others (1996) because they developed a full set of attenuation relations based on data primarily from Europe but also including several earthquakes from Iran. The relations for PGA from Zare and Bard (1999) and Ambraseys and others (1996) have a similar form and, within about 5 km of the fault, tend to bracket the attenuation relations developed for earthquakes in western North America.

In addition to the Ambraseys and others (1996) ground-motion relations, we use four western North America relations: Abrahamson and Silva (1997) for rock and reverse-oblique slip, Boore and others (1997) for V_s30=760 and mixed reverse- and strike-slip faulting, Sadigh and others (1997) for rock and mixed reverse- and strike-slip faulting, and Campbell and Bozorgnia (2003) for firm-rock and mixed reverse- and strike-slip faulting. Several of these relations are presented in figure 5. To account for modeling uncertainty, we combine the ground-motion estimates in a logic tree, giving 60-percent weight to the western North America group and 40-percent weight to the Ambraseys relation.

Deeper Earthquakes

To estimate ground motions for intermediate-depth seismicity (50–250 km), we use empirical relations developed from subduction-environment earthquakes. We use a relation developed by Atkinson and Boore (2003) for earthquakes from 50- to 100-km depth (in-slab, all data, V_s30=760 site condition) and a relation developed by Youngs and others (1997) for earthquakes from 50- to 250-km depth (in-slab, rock site condition), both being weighted equally between 50- and 100-km depth. Afghanistan is one of the few places on Earth where continental earthquakes as deep as 200 km or more are known to cause damage, but we have little strong-motion data to guide ground-motion predictions for such earthquakes. For

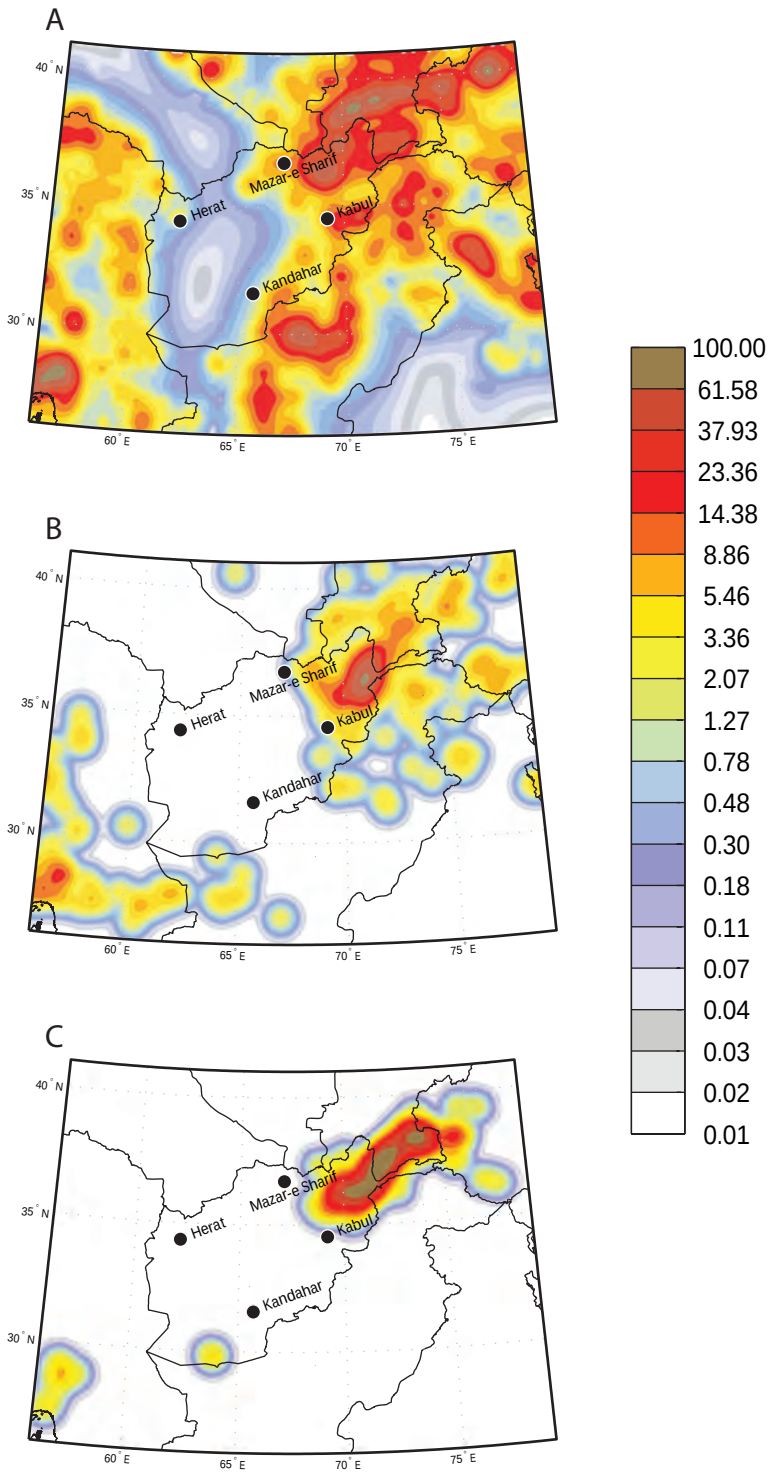

Figure 3. Maps of modeled earthquake rates derived from smoothed seismicity showing the number of M6.0 earthquakes occurring per 10,000 km^2 per 10,000 years for (A) 0–50 km depth, (B) 50–100 km depth and (C) 100–250 km depth.

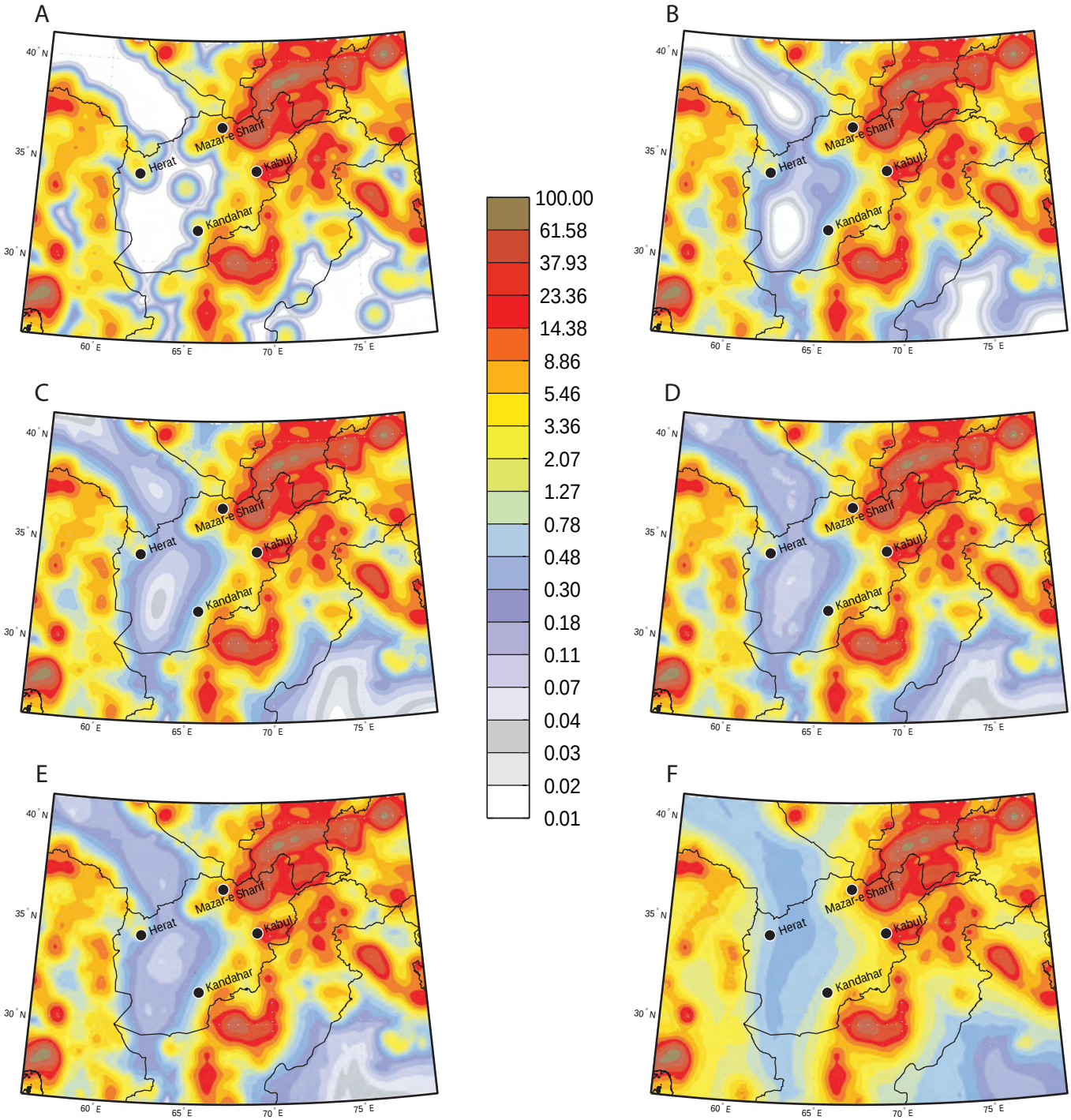

Figure 4. Maps showing the number of M6.0 earthquakes occurring per 10,000 km^2 per 10,000 years between 0 and 50-km depth and the effect of various smoothing parameters (see text); (A) constant smoothing width of 50 km as is used in the national seismic hazard maps of the United States, (B) smoothing width from 50 to 100 km with at least three earthquakes, (C) smoothing width from 50 to 150 km with at least three earthquakes, (D) smoothing width from 50 to 200 km with at least three earthquakes, (E) smoothing width from 50 to 500 km with at least three earthquakes, and (F) smoothing width from 50 to 500 km with at least 10 earthquakes.

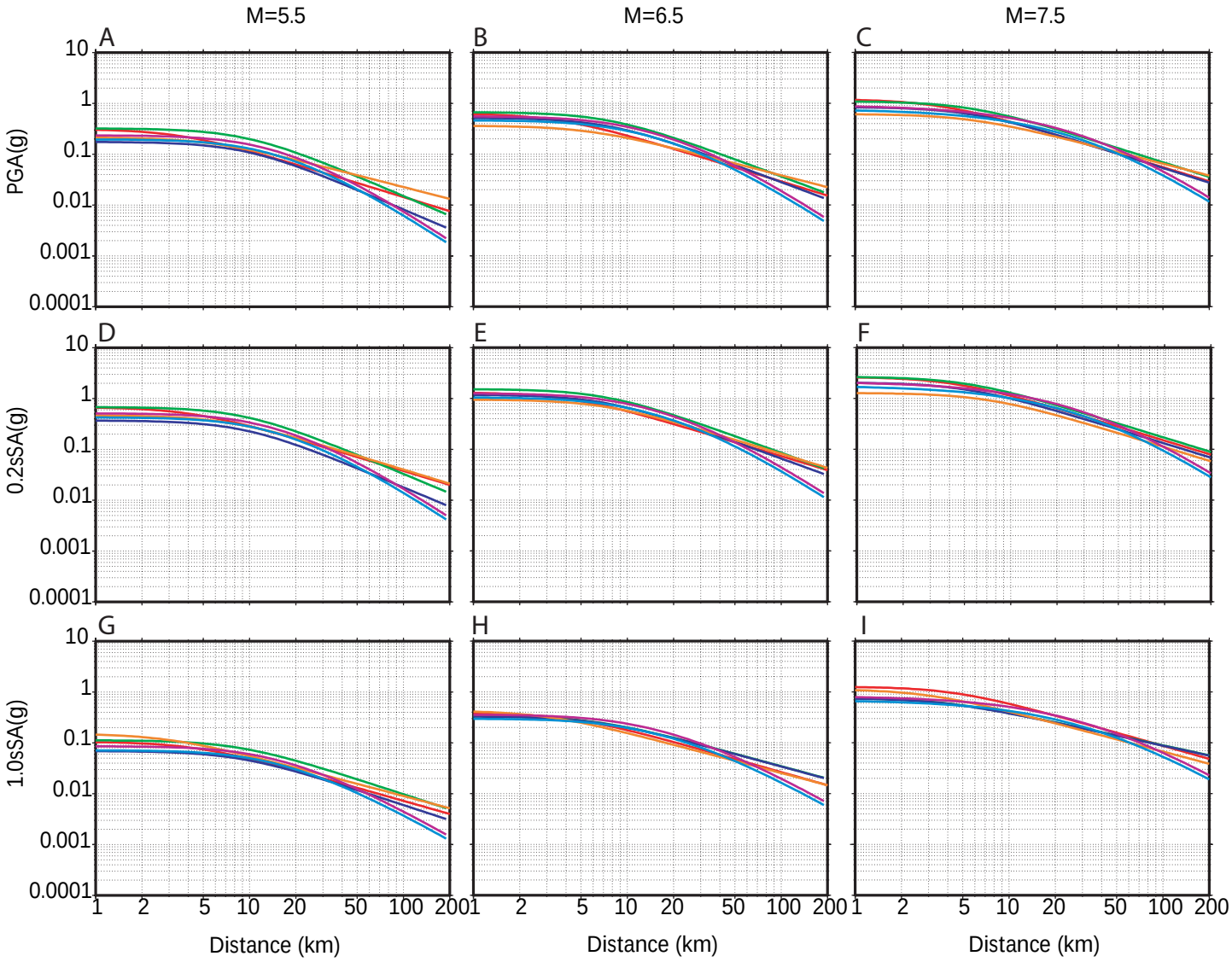

Figure 5. Median ground motions from selected ground-motion relations at three magnitudes for (A, B, C) Peak Ground Acceleration (PGA); (D, E, F) 0.2-second Spectral Acceleration (SA); and (G, H, I) 1.0-second SA. The cyan curve is from Sadigh and others (1997) (strike slip, soft rock); magenta is from Sadigh and others (1997) (reverse slip, soft rock); orange is from Boore and others (1997) (all and unknown slip, 620 m/s); blue is from Abrahamson and Silva (1997) (strike slip, rock and shallow soil); green is from Abrahamson and Silva (1997) (reverse slip, rock and shallow soil); and red is from Ambraseys and others (1996) (360<v<750).

a site directly above the March 2002 Hindu Kush earthquake (moment-magnitude = 7.4 and depth = 200 km), the relation of Youngs and others (1997) would predict a median peak acceleration of 10 percent *g* for a rock site and 18 percent *g* for a soil site. These levels of ground motion are judged to be reasonable for the damage (Grunthel and others, 1998; Wald and others, 1999) and triggering of landslides (Harp and Wilson, 1995) observed from the 2002 earthquake. Thus, in the absence of quantitative evidence to the contrary, we accept these relations as reasonable predictions of strong ground motion from Afghanistan's deep earthquakes.

Earthquake Hazard

For a given site, the hazard calculation considers the magnitude, rate, and location of each modeled earthquake, computes the earthquake-to-site distance, and uses the predicted ground motion for that magnitude and distance and its variability to compute the rates at which specified levels of motion are exceeded (for example, Frankel and others, 1996; Appendix). These rates are summed over all sources to get the hazard curve, the functional relationship between exceedance rate and ground motion, for the given site. An acceptable hazard level

for design is selected (say, 2 percent or 10 percent probability of exceedance in 50 years, which is generally an engineering decision), and the corresponding ground-motion level is computed from the hazard curve. Ground-motion values from many sites (~35,000 for the Afghanistan study area) are plotted at the site locations and contoured to generate a seismic hazard map.

Hazard Curves

In figure 6, we present "partial" and total hazard curves for four cities within Afghanistan: Kabul, Mazar-e Sharif, Herat, and Kandahar. The partial curves show contributions from individual elements of the source model, like a particular fault or seismicity in a particular depth range. These curves show the annual probability of exceedance on the y-axis relative to three measures of ground motion on the x-axis. Probabilistic ground motions with exceedance probabilities of 2 percent and 10 percent in 50 years are presented in table 2. From the hazard curves we find that the shallow instrumental-seismicity model is the primary contributor to seismic hazard at most of these sites. The city of Kabul borders on the Chaman fault, and as a result, large earthquakes on the fault make a significant contribution to the probable ground motions for the city, especially at 1-second SA. Of the four cities considered, Herat has the least contribution to ground motion from intermediate-depth seismicity. It also has the greatest relative contribution from seismicity specified on specific fault sources.

Hazard Maps

Figures 7 through 10 show maps of probabilistic PGA, 0.2-second SA and 1-second SA for 2-percent and 10-percent probability of exceedance in 50 years for fault sources and three smoothed-seismicity subsets. Figure 11, plate 1, and plate 2 present the combined effect of all sources. Western Afghanistan has low seismic hazard relative to the east. Along much of eastern Afghanistan and particularly in the northeast, faults and background seismicity both contribute to the hazard. Southward along the border with Pakistan, the contribution from seismicity deeper than 50 km disappears, but shallow seismicity remains significant.

Of the major cities in Afghanistan, Kabul has by far the greatest seismic hazard, primarily due to its proximity to the potentially fast-moving Chaman fault. The estimated PGA value of 50 percent *g* for 2 percent in 50 years is comparable to the seismically active regions of the intermountain west in the United States. Northeast of Kabul, the modeled faults and high rates of background seismicity combine to give hazard values approaching those found in some seismically active regions of California. The hazard in Mazar-e Sharif has about one-half that in Kabul, largely because it is far removed from concentrated sources of seismicity. Herat lies close to the Hari Rud fault. Because of this fault's low slip rate, large earthquakes are infrequent, so Herat has a relatively higher hazard for low return periods (for example, 2-percent chance of exceedance in 50 years) but lower hazard for short return periods (for example, 10-percent chance of exceedance in 50 years). Herat is the one location in Afghanistan where our analysis based on instrumental seismicity may underestimate what might be expected from the historical catalog. Kandahar, being located in southeastern Afghanistan, is farther removed from much of the continental convergence taking place in the northeast. Moreover, Kandahar is located well away from the Chaman fault, further decreasing its seismic hazard. Transportation and lifeline infrastructure between Kabul and Kandahar, however, are at significant risk if the infrastructure is built along or crosses the Chaman fault. The infrastructure that extends from Herat to Kabul is at relatively reduced risk since the slip rate of the Hari Rud fault is a factor of 5 less than that of the Chaman.

Table 2. Probabilistic ground motions for selected cities.

			2%			10%		
			Probability of exceedance in 50 years					
City	Lat.	Long.	PGA (%g)	0.2 sec	1.0 sec	PGA	0.2 sec	1.0 sec
Kabul	34.53	69.17	48	113	53	25	57	22
Mazar-e Sharif	36.70	67.10	33	78	22	16	37	11
Herat	34.35	62.18	28	62	24	7	15	4
Kandahar	31.61	65.69	13	30	16	7	16	8

Figure 6. (facing page) Hazard curves for Kabul (A, B, C), Mazar-e Sharif (D, E, F), Herat (G, H, I), and Kandahar (J, K, L) for PGA (A, D, G, J), 0.2-second SA (B, E, H, K), and 1.0-second SA (C, F, I, L). The horizontal dashed black lines correspond to a 10- (upper) and 2- (lower) percent probability of exceedance in 50 years or a return period of about 500 and 2,500 years, respectively. The solid black line is the seismic hazard curve resulting from a combination of all sources. The dashed-dot curves reflect contributions to seismic hazard using the ground-motion relation of Ambraseys and others (1996), while the solid curves represent Western United States ground-motion relations. The red curves are the contribution to seismic hazard from fault sources that are characteristic, and the green curves are for Gutenberg-Richter. The blue curves represent contributions from background seismicity less than 50-km depth, while the cyan curves represent contributions from seismicity between 50- and 100-km depth (solid) and 100- and 250-km depth (dashed-dot).

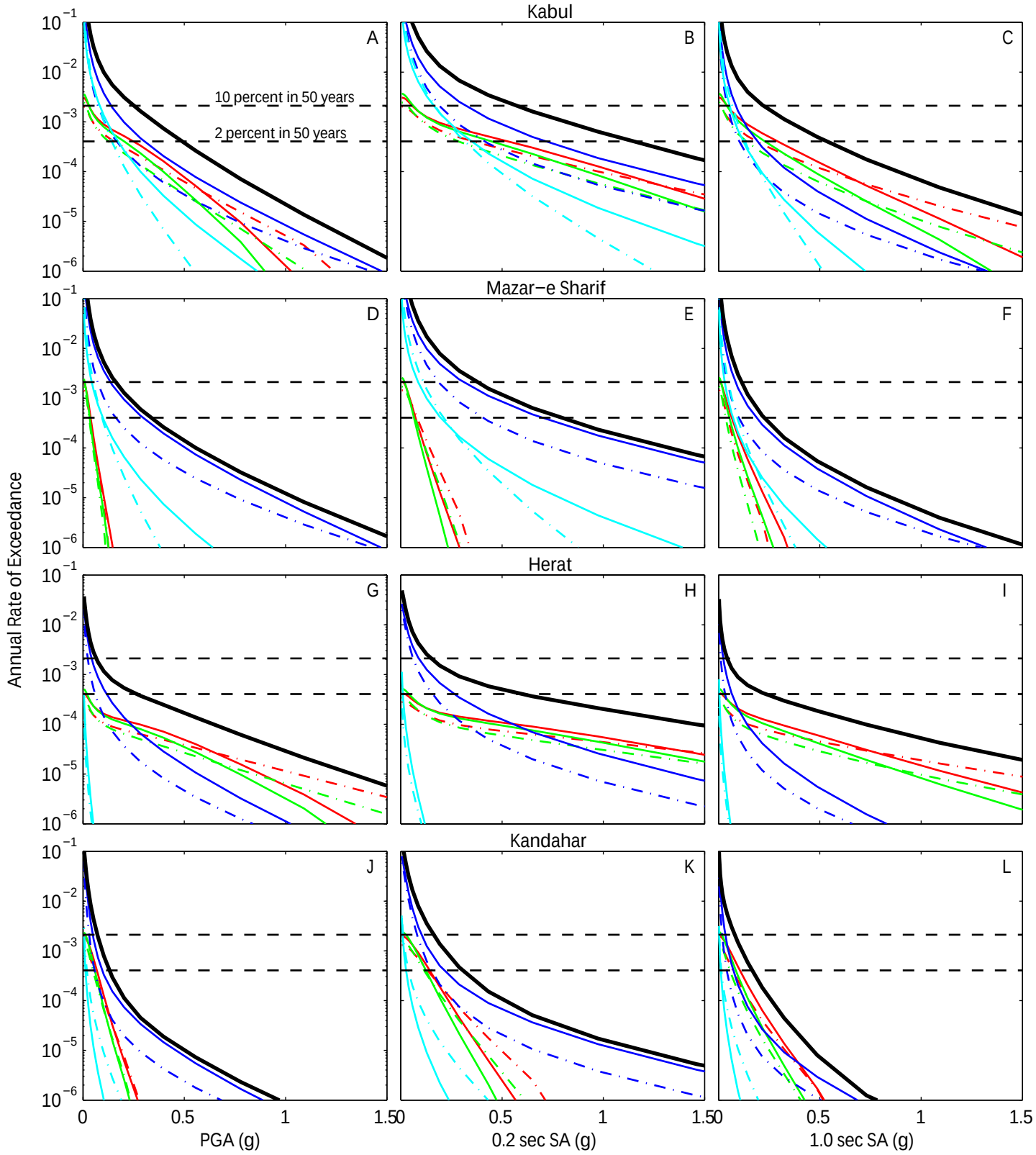
Kabul
Mazar−e Sharif
Herat
Kandahar
A
B
C
D
E
F
G
H
I
J
K
L
10 percent in 50 years
2 percent in 50 years
Annual Rate of Exceedance
PGA (g)
0.2 sec SA (g)
1.0 sec SA (g)

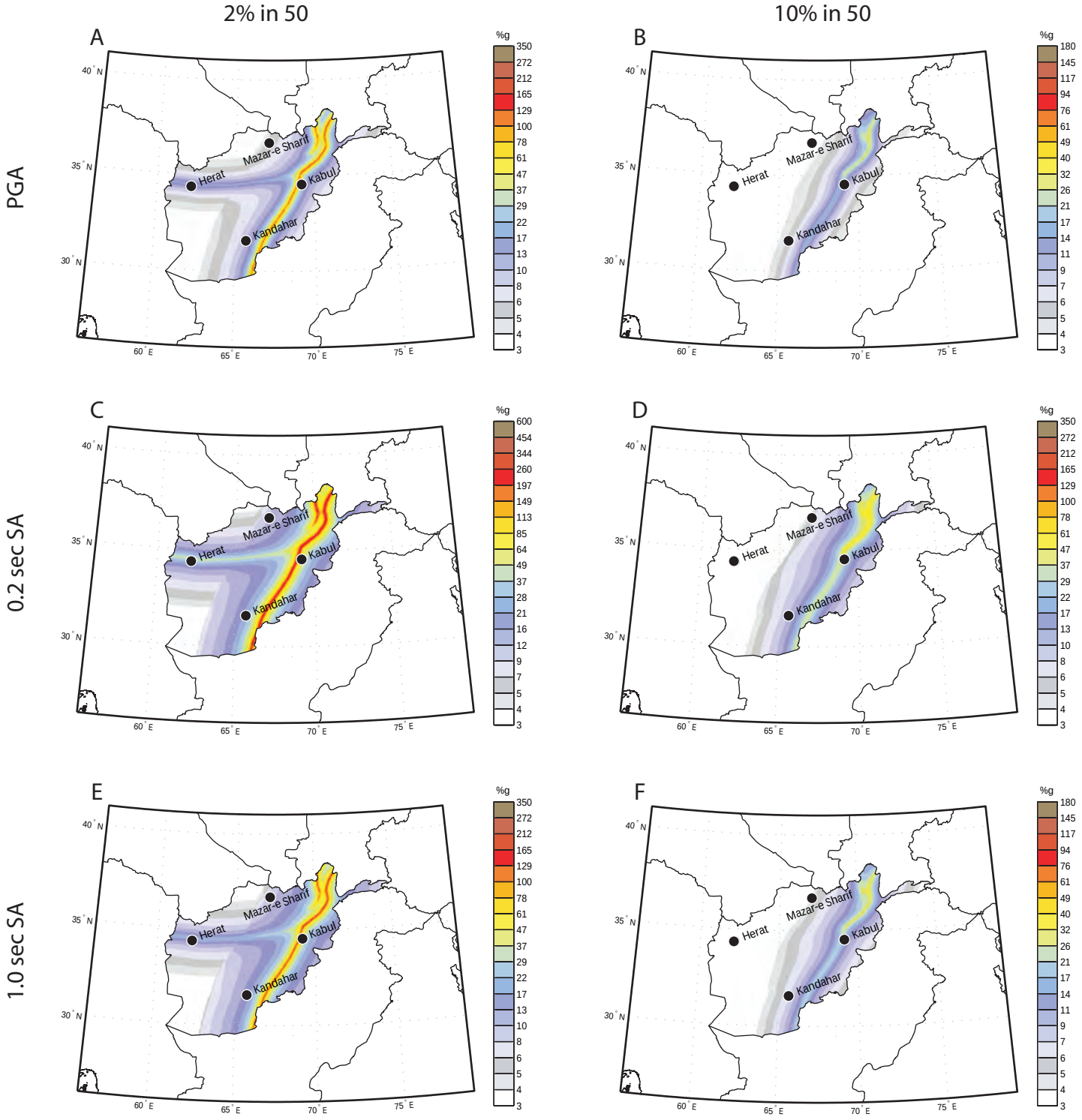

Figure 7. Ground motions for fault sources for PGA (A, B), 0.2-second SA (C, D), and 1.0-second SA (E, F) at 2-percent (A, C, E) and 10-percent (B, D, F) probability of exceedance in 50 years.

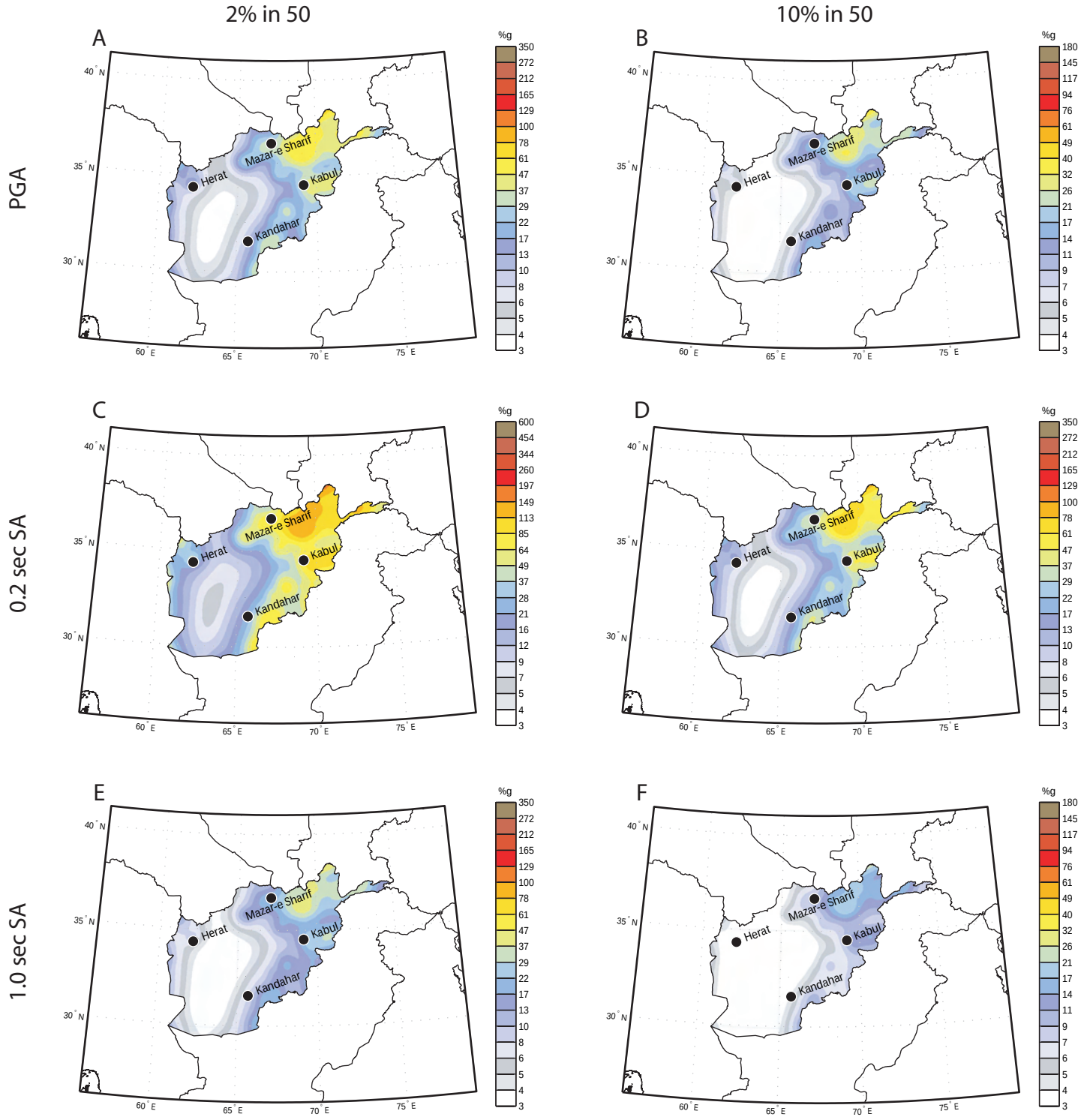

Figure 8. Ground motions for smoothed seismicity between 0- and 50-km depth for PGA (A, B), 0.2-second SA (C, D), and 1.0-second SA (E, F) at 2-percent (A, C, E) and 10-percent (B, D, F) probability of exceedance in 50 years.

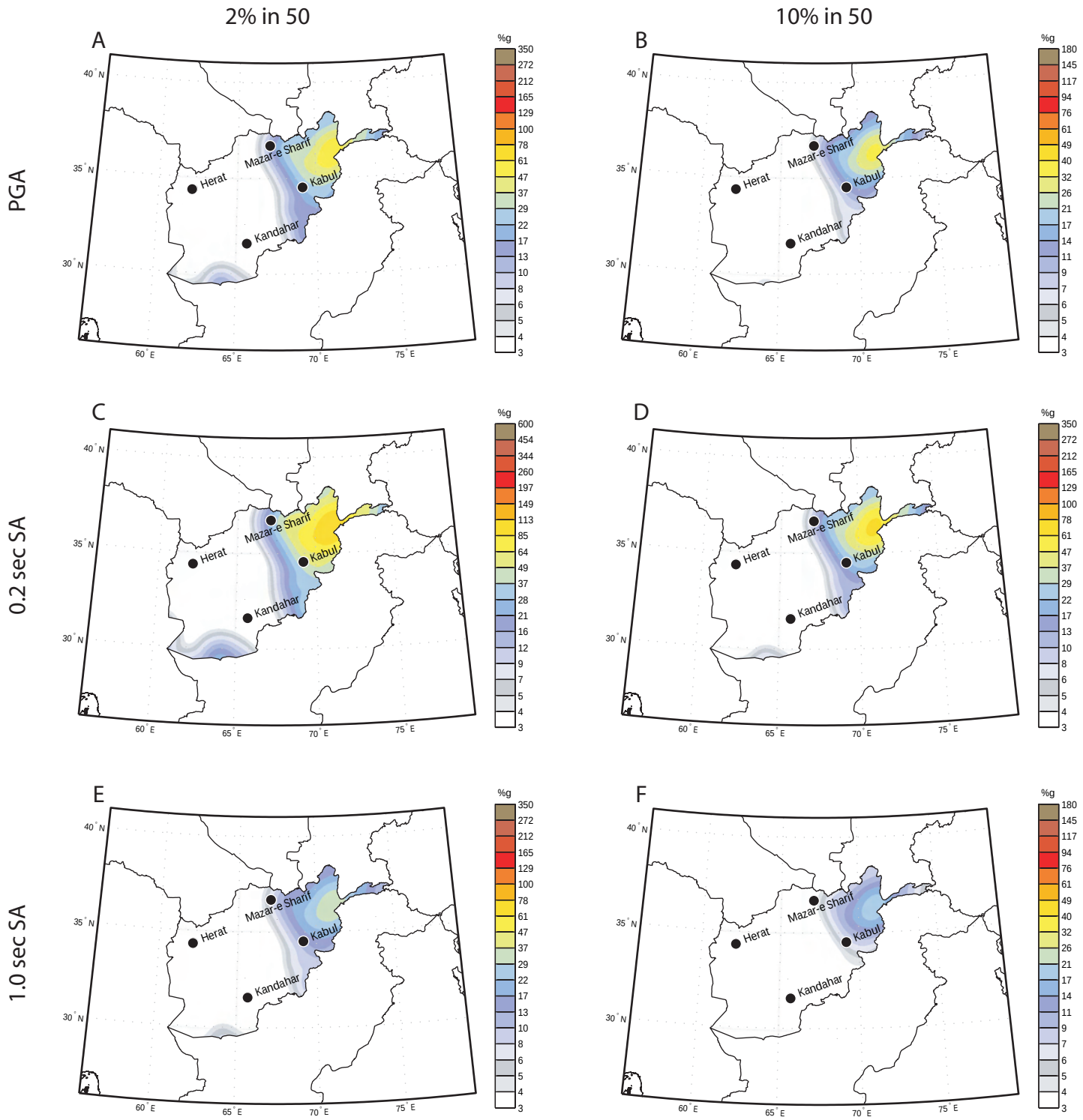

Figure 9. Ground motions for smoothed seismicity between 50- and 100-km depth for PGA (A, B), 0.2-second SA (C, D), and 1.0-second SA (E, F) at 2-percent (A, C, E) and 10-percent (B, D, F) probability of exceedance in 50 years.

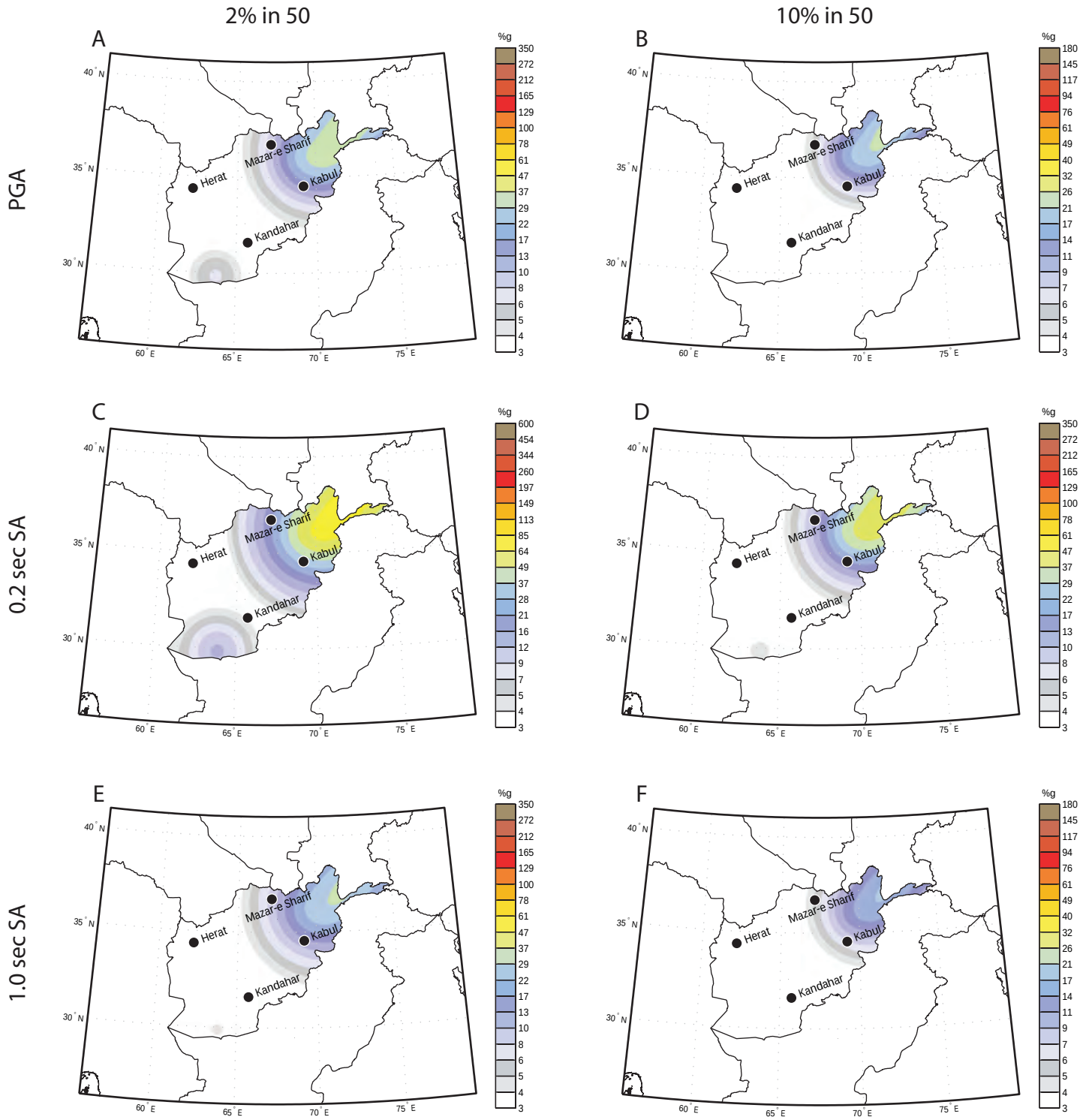

Figure 10. Ground motions for smoothed seismicity between 100- and 250-km depth for PGA (A, B), 0.2-second SA (C, D), and 1.0-second SA (E, F) at 2-percent (A, C, E) and 10-percent (B, D, F) probability of exceedance in 50 years.

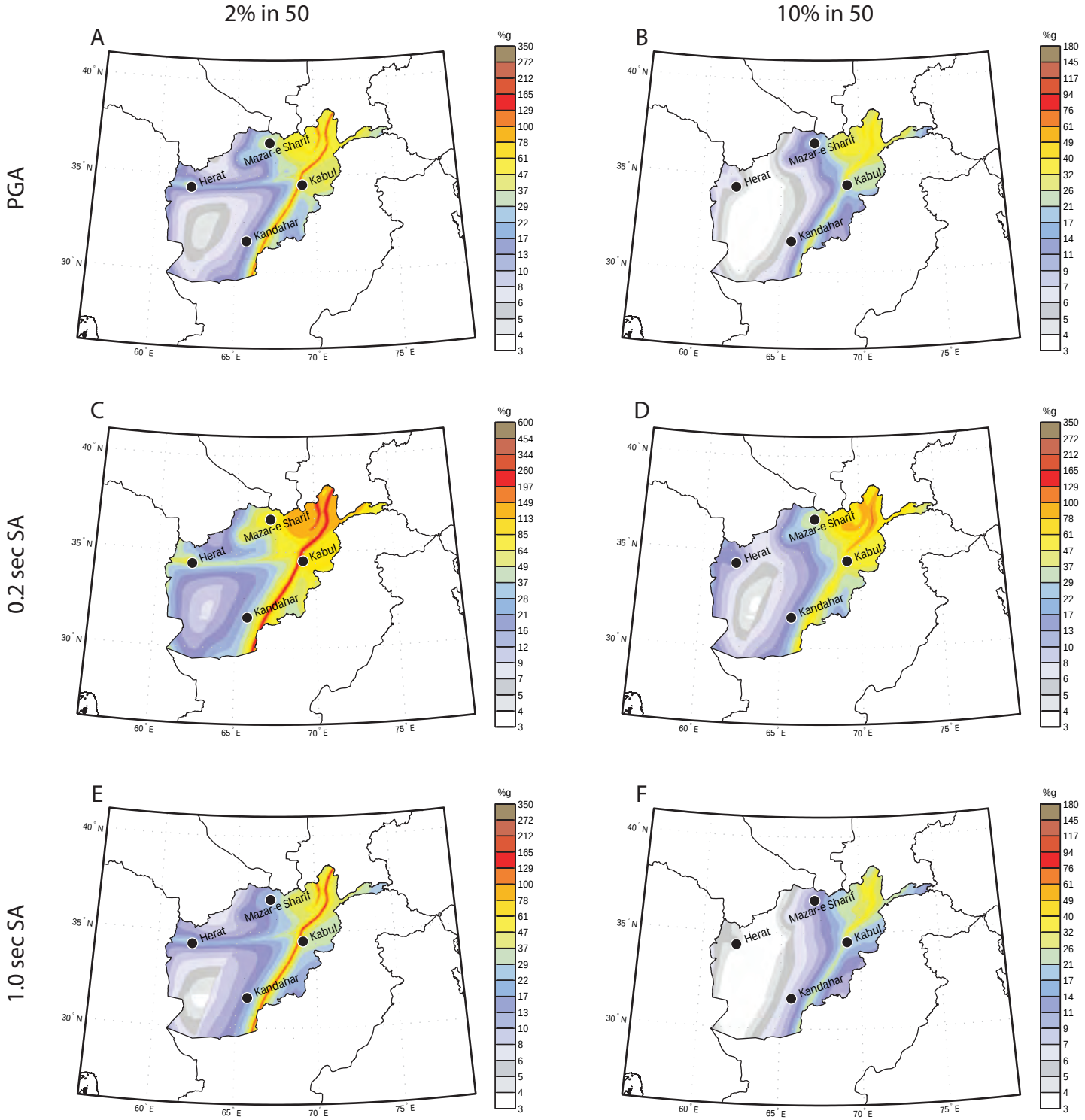

Figure 11. Ground motions for all modeled sources for PGA (A, B), 0.2-second SA (C, D), and 1.0-second SA (E, F) at 2-percent (A, C, E) and 10-percent (B, D, F) probability of exceedance in 50 years.

Conclusions

Several sources of seismicity are present in Afghanistan and contribute to appreciable seismic hazard for several major cities including Kabul, Mazar-e Sharif, and Herat. We estimate that Kabul, Mazar-e Sharif, Herat, and Kandahar have a 2-percent chance in 50 years of exceeding a peak ground acceleration of 50, 35, 28, and 13 percent *g* respectively, and a 10-percent chance in 50 years of exceeding a peak ground acceleration of 27, 17, 7, and 7 percent *g*, respectively. These values are similar to values found for the intermountain West of the United States. However, the hazard values for Afghanistan are relatively uncertain owing to a lack of information characterizing the sources of seismic hazard, particularly the many faults that might be active. Future studies should concentrate on identifying active faults and estimating their slip rates, likely magnitudes, and recurrence rates. Additional work should be performed on known faults such as the Chaman and Hari Rud to better constrain the aforementioned parameters. Further improvements in a seismic-hazard analysis for Afghanistan could be made by making ground-motion relations specific to Afghanistan rather than relying on estimates made for tectonically analogous regions of the United States and Europe.

Acknowledgments

We gratefully acknowledge the reviews and input of Rob Wesson, Rus Wheeler, and Tony Crone. Additional input from Cal Ruleman and Kathy Haller was appreciated. This work was supported by the U.S Geological Survey's Afghanistan Project, which is funded by the U.S. Agency for International Development aid in Kabul through Interagency Agreement 306-P-00-04-00566-00.

References Cited

Abrahamson, N.A., and Silva, W.J., 1997, Empirical response spectral attenuation relations for shallow crustal earthquakes: Seismological Research Letters, v. 68, p. 94–127.

Ali, Q., 2005, World housing encyclopedia report on Pakistan: Earthquake Engineering Research Institute, p. 35.

Ambraseys, N., and Bilham, R., 2003, Earthquakes in Afghanistan: Seismological Research Letters, v. 42, no. 2, p. 107–123, and electronic supplement.

Ambraseys, N.N., Simpson, K.A., and Bommer, J.J., 1996, Prediction of horizontal response spectra in Europe: Earthquake Engineering and Structural Dynamics, v. 25, p. 371–400.

Atkinson, G.M., and Boore, D.M., 2003, Empirical ground-motion relations for subduction zone earthquakes and their applications to Cascadia and other regions: Bulletin of the Seismological Society of America, v. 93, p. 1703–1729.

Bergman, E.A., 2006, Chapter B—A comprehensive earthquake catalogue for the Afghanistan region, *in* Dewey, J.W., ed., Seismicity of Afghanistan and Vicinity, U.S. Geological Survey Open-File Report 2006–1185, 60 p.

Boore, D.M., Joyner, W.B., and Fumal, T.E., 1997, Equations for estimating horizontal response spectra and peak acceleration from western North American earthquakes—a summary of recent work: Seismological Research Letters, v. 68, p. 128–153.

Campbell, K.W., and Bozorgnia, Y., 2003, Updated near-source ground motion (attenuation) relations for the horizontal and vertical components of peak ground acceleration and acceleration response spectra: Bulletin of the Seismological Society of America, v. 93, p. 314–331.

Dewey, J.W., Bergman, E.A., Hopper, M.G., and Sipkin, S.A., 2006, Chapter A—Overview of the seismicity of Afghanistan, *in* Dewey, J.W., ed., Seismicity of Afghanistan and vicinity, U.S. Geological Survey Open-File Report 2006–1185, 60 p.

Ellsworth, W.L., 1990, Earthquake history, 1769–1989, *in* Wallace, R.E., ed., The San Andreas fault system, California: U.S. Geological Survey Professional Paper 1515, p. 152–187.

Frankel, A., Mueller, C., Barnhard, T., Perkins, D., Leyendecker, E., Dickman, N., Hanson, S., and Hopper, M., 1996, National seismic-hazard maps—Documentation June 1996: U.S. Geological Survey Open-File Report, v. 96–532, p. 110.

Gardner, J.K., and Knopoff, L., 1974, Is the sequence of earthquakes in southern California, with aftershocks removed, Poissonian?: Bulletin of the Seismological Society of America, v. 64, p. 1363–1367.

Grunthel, G., Musson, R., Schwarz, J., and Stucchi, M., 1998, European Macroseismic Scale (EMS-98): Luxembourg, Conseil de l'Europe, v. 7.

Haeussler, P.J., Schwartz, D.P., Dawson, T.E., Stenner, H.D., Lienkaemper, J.J., Sherrod, B., Cinti, F.R., Montone, P., Craw, P.A., Crone, A.J., and Personius, S.F., 2004, Surface rupture and slip distribution of the Denali and Totschunda faults in the 3 November 2002 M 7.9 earthquake, Alaska: Bulletin of the Seismological Society of America, v. 94, no. 6B, p. S23–S52.

Harp, E.L., and Wilson, R.C., 1995, Shaking intensity thresholds for rock falls and slides—Evidence from 1987 Whittier Narrows and Superstition Hills earthquake strong-motion records: Bulletin of the Seismological Society of America, v. 85, no. 6, p. 1739–1757.

Lawrence, R.D., Hasan Khan, S., and Nakata, T., 1992, Chaman Fault, Pakistan-Afghanistan, *in* Bucknam, R.C., and Hancock, P.L., eds., Major active faults of the world—Results of IGCP Project 206: Annales Tectonicae, Special Issue Supplement to v. 6, p. 196–223.

Lawson, A.C., 1908, The California Earthquake of April 18, 1906—Report of the State Earthquake Investigation Commission: Carnegie Institution of Washington Publication, v. 87.

Quittmeyer, R.C., and Jacob, K.H., 1979, Historical and modern seismicity of Pakistan, Afghanistan, northwestern India, and southeastern Iran: Bulletin of the Seismological Society of America, v. 69, no. 3, p. 773–823.

Reiter, Leon, 1990, Earthquake Hazard Analysis: Issues and Insights: New York, Columbia University Press, 254 p.

Richter, C.F., 1958, Elementary seismology: San Francisco, W.H Freeman and Company, 768 p.

Ruleman, C.A., Crone, A.J., Machette, M.N., Haller, K.M., and Rukstales, K., 2007, Map and database of probable and possible quaternary faults in Afghanistan: U.S. Geological Survey Open-File Report, v. 2007–1103, 45 p.

Sadigh, K., Chang, C.-Y., Egan, J.A., Makdisi, F., and Youngs, R.R., 1997, Attenuation relationships for shallow crustal earthquakes based on California strong motion data: Seismological Research Letters, v. 68, p. 180–189.

Sborshchikov, I.M., Savostin, L.A., and Zonenshayn, L.P., 1981, Present plate tectonics between Turkey and Tibet: Tectonophysics, v. 79, p. 45–73.

Sieh, K., 1978, Slip along the San Andreas Fault associated with the great 1857 earthquake: Bulletin of the Seismological Society of America, v. 68, no. 4, p. 1421–1448.

Sipkin, S.A., 2003, A correction to body-wave magnitude mb based on moment magnitude Mw: Seismological Research Letters, v. 74, p. 739–742.

Tapponnier, P., Mattauer, M., Proust, F., and Cassaigneau, C., 1981, Mesozoic ophiolites, sutures, and large-scale tectonic movements in Afghanistan: Earth and Planetary Science Letters, v. 52, p. 355–371.

Townley, S.D., 1939, Earthquakes in California, 1769 to 1928: Bulletin of the Seismological Society of America, v. 29, no. 1, p. 21–252.

Trifonov, V.G., 1978, Late Quaternary tectonic movements of western and central Asia: Geological Society of America Bulletin, v. 89, p. 1059–1072.

Utsu, T., 2002, Relationships between magnitude scales, *in Lee, W.H.K, Kanamori, H., Jennings, P.C., and Kisslinger, C. ed.,* International Handbook of Earthquake and Engineering Seismology: Academic Press, p. 733–746.

Wald, D.J., Quitoriano, V., Heaton, T.H., and Kanamori, H., 1999, Relationships between peak ground acceleration, peak ground velocity, and modified Mercalli Intensity in California: Earthquake Spectra, v. 15, no. 3, p. 557–564.

Weichert, D.H., 1980, Estimation of earthquake recurrence parameters for unequal observation periods for different magnitudes: Bulletin of the Seismological Society of America, v. 70, p. 1337–1356.

Wellman, H.W., 1965, Active wrench faults of Iran, Afghanistan and Pakistan: Geologische Rundschau, v. 55, no. 3, p. 716–735.

Wells, D.L., and Coppersmith, K.J., 1994, New empirical relationships among magnitude, rupture length, rupture width, rupture area, and surface displacement: Bulletin of the Seismological Society of America, v. 84, no. 4, p. 974–1002.

Wheeler, R.L., Bufe, C.G., Johnson, M.L., and Dart, R.L., 2005, Seismotectonic map of Afghanistan, with annotated bibliography: U.S. Geological Survey Open-File Report 2005-1264, p. 34.

Wood, H.O., and Neumann, F., 1931, Modified Mercalli intensity scale of 1931: Bulletin of the Seismological Society of America, v. 21, p. 277–283.

Yeats, R.S., Lawrence, R.D., Jamil-Ud-Din, S., and Khan, S.H., 1979, Surface effects of the 16 March 1978 earthquake, Pakistan-Afghanistan border, *in* Farah, A., and De Jong, K.A., eds., Geodynamics of Pakistan: Quetta, Pakistan, Geological Survey of Pakistan, p. 359–361.

Youngs, R.R., Chiou, S.-J., Silva, W.J., and Humphrey, J.R., 1997, Strong ground motion attenuation relationships for subduction zone earthquakes: Seismological Research Letters, v. 68, p. 58–73.

Zare, M., and Bard, P.Y., 1999, Attenuation of peak ground motion in Iran, in Congrès Génie parasismique et réponse dynamique des ouvrages, 5th National Conference, France.

Glossary

***a*-value** In an exponential relationship that describes the annual frequency, *N*, of earthquakes with magnitude greater than or equal to *M*, also called the Gutenberg-Richter relationship, which is defined to be $\log(N(M))=a-bM$, the *a*-value represents the log of frequency of earthquakes that occur with magnitude greater than or equal to zero.

Aftershocks Earthquakes that occur after a mainshock, have a smaller magnitude, and occur near the mainshock.

***b*-value** In an exponential relationship that describes the frequency of earthquakes with a given magnitude (see *a*-value), the *b*-value represents the slope of this relationship or the relative frequency of different magnitudes. For example, a *b*-value of 1 means that a magnitude 5 occurs 10 times as often as a magnitude 6.

Body-wave magnitude (m_b) A magnitude that is measured using the first teleseismic P body-wave.

Correlation distance The spatial distance over which a parameter of interest is correlated. This term is used in conjunction with the smoothing distance.

Decluster The process of declustering removes aftershocks and foreshocks from seismic catalogs. This is necessary to produce a catalog that contains independent earthquakes, which is required for time-independent hazard analysis.

Earth structure model A model describing the structure of the Earth in terms of seismic velocity, rheology, temperature, composition, and so forth.

5-percent-damped single-degree-of-freedom oscillator A simple representation of a structure used to estimate its response.

Epistemic uncertainty Uncertainty relating to a lack of knowledge about the basic underlying process. This form of uncertainty can be reduced through research.

Foreshocks Earthquakes that precede a mainshock, have a smaller magnitude, and occur near the mainshock.

Ground motion The vibratory movement of the ground resulting from an earthquake.

Ground-motion relations Equations that predict earthquake ground motions as a function of distance, magnitude, and sometimes other variables. Ground motion generally depends on the tectonic environment: active or stable, crustal or subduction. In the simplest models, shaking is predicted as a function only of earthquake magnitude, earthquake-to-site distance, and, perhaps site condition (for example, rock or soil category). More sophisticated models might also include style of faulting, depth of faulting, better site descriptors like V_s30, and other predictor variables.

Hazard curve The functional relationship between exceedance frequency and ground motion.

Left-lateral strike-slip fault A fault across which geologic features are displaced such that when looking across the fault, the far side is displaced to the left.

Logarithmic scale A scale in which the logarithm of the quantity is the desired unit.

Logic tree To account for uncertainty, results from alternative hazard model elements are weighted and summed in the final analysis.

Instrumental catalog A compiled list of earthquakes derived from seismographs generally containing the earthquake location, origin time, and magnitude.

Magnitude A logarithmic value that represents the size of an earthquake. An increase of one magnitude unit reflects a ~tenfold increase in seismic-wave amplitude.

Magnitude saturation The phenomenon in which the measurement device or method is not sensitive above a certain magnitude. Different magnitude scales, for example, body-wave magnitude and surface-wave magnitude, have different magnitudes at which the scale saturates.

Mainshock The largest earthquake in a series.

Mean The average value, $\propto$, from a set of *n* observations, x_i, defined by the equation

$$\mu = \frac{1}{n}\sum_{i=1}^{n} x_i \ .$$

Median For a distribution of values, the median represents the middle value or the 50th percentile.

Modified Mercalli Intensity An earthquake scale that describes the effects of various earthquake ground motion intensities.

Moment budget The seismic moment available that can be released in a certain size and number of earthquakes over a period of time.

Moment magnitude (M_w) A magnitude scale that is derived from the seismic moment.

Normal distribution A distribution of random values with a probability density function, *f(x)*, described by the equation

$$f(x) = \frac{1}{\sigma\sqrt{2\pi}} e^{-\frac{(x-\mu)^2}{2\sigma^2}}$$

where μ is the mean and σ is the standard deviation.

Normalization To divide a parameter by a common value.

Origin time The time at which an earthquake occurred, usually given in universal time.

Recurrence time The average amount of time between earthquake occurrences at a location.

Return period The inverse of the annual exceedance rate. For example, a 10-percent probability of exceedance in 50 years corresponds to an annual rate of exceedance of 0.0021 or a return period of 475 years.

Right-lateral strike-slip fault A fault across which geologic features are displaced such that when looking across the fault, the far side is displaced to the right.

Seismic hazard The rate of exceeding a potential ground motion that can be expected from a seismic source.

Seismic hazard model A model that is used to compute the seismic hazard at a particular location from multiple earthquake sources.

Seismic risk The social and economic consequences of seismic ground motion.

Seismic moment A quantity that is related to the size of an earthquake. It is equal to the product of fault area, fault slip, and fault rigidity or shear modulus.

Seismic source This term can be considered synonymous with an earthquake source such as faults and subduction zones.

Seismograph An instrument capable of recording ground motions, typically produced by earthquakes.

Shear-wave A type of ground motion produced by an earthquake in which particle motion is perpendicular to the direction of the propagating wave.

Site condition A representation of the site at which ground motions are calculated, for example, rock or soil. The site condition can be characterized by averaging the shear-wave seismic velocity over a specified depth, generally the top 30 meters.

Slip rate The long-term rate at which each side of a fault moves past each other.

Smoothing kernel A function that averages values over some region. Typically, a Gaussian distribution is used for the functional form of the smoothing kernel.

Spectral acceleration The peak response of a damped (usually 5 percent damping), single-degree-of-freedom oscillator, with a specific natural period, to ground shaking; this measure of shaking is often preferred by structural engineers because it simulates the response of a simple building.

Standard deviation The average deviation from the mean, $\propto$, of n observations, x_i, defined by the equation

$$\sigma = \sqrt{\frac{1}{n}\sum_{i=1}^{n}\left(x_i - \mu\right)^2} \; .$$

Surface rupture The break on the ground surface at the top of a fault that occurred as a result of an earthquake.

Surface-wave magnitude (M_s) A magnitude scale that is derived from the teleseismic surface-waves, which are seismic waves that move along the surface of the earth.

Teleseismic Distances between an earthquake and an observer that are greater than 1,000 kilometers.

Time-and-distance window A period of time before and after an earthquake and an area surrounding an earthquake in which foreshocks and aftershocks are located and removed from an earthquake catalog.

Transpressional A tectonic environment in which the crust is being both sheared and shortened.

Truncated exponential An exponential distribution that is truncated at an upper and lower limit.

V_s30 The average seismic shear wave velocity of the upper 30 meters of the Earth's surface at a given location.

Vulnerability curve A function that relates ground motion to the expected amount of damage a structure will sustain.

Wave propagation The movement of a seismic wave through the earth.

Appendix: Primer on Probabilistic Seismic-hazard Analysis

Introduction

In probabilistic seismic hazard analysis (PSHA), we are interested in knowing the probability of exceeding a certain amount of ground motion within a specific period of time. For most structural applications, we find that knowing the ground motion that is exceeded with a 2-percent and 10-percent probability in 50 years yields an acceptable level of risk. These probability levels correspond to annual rates of exceedance of 0.000404 and 0.0021, respectively, and are given by the equation, $-\ln(1-Pe)/T$, where Pe is the probability level and T is the time period. These probability levels or annual rates of exceedance are derived from a seismic-hazard curve (for example, fig. 6 for Kabul), which plots the annual rate of exceedance relative to ground motion. To generate this curve at a particular site, we need to sum for each potential earthquake source and ground-motion level the product of (1) the annual rate of the earthquake and (2) the probability that it will, having occurred, exceed the defined level of ground motion at the site. In the following sections we explain how seismic sources are defined and rates are derived, the first part of the above calculation. We then explain ground-motion relationships, which is relevant to the second part of the above calculation. We conclude by giving the reader an appreciation for how the ground motions can be converted to seismic intensity, a measure of the damage likely to be sustained given the resulting ground motions. For a more thorough description of seismic hazard analysis, please see the book entitled “Earthquake Hazard Analysis” by Leon Reiter (1990).

Earthquake Sources

The first step in PSHA is to identify the seismic sources. At the most basic level, seismic sources are active faults. Yet not all active faults are explicitly included in the analysis because their rates of activity cannot be quantified. We therefore have two basic ways to include active faults as seismic sources. Either active faults are included explicitly when their geometry is known and a slip rate can be assigned, or faults are inferred to be active in a source area that has seismicity. For the latter case the rate of seismicity is used to quantify the seismic source without characterizing any individual faults. This kind of source is considered “smoothed seismicity” since earthquakes are spread over a region, typically with a 50-km smoothing kernel or uniformly in an areal source zone.

Earthquake Rates

The next step in PSHA is to define the rates of earthquakes on each of these sources. For example, consider the Chaman fault to be a characteristic fault with a slip rate of 10 mm/yr and a characteristic earthquake size of M_w 7. Characteristic behavior means that the fault regularly ruptures in an earthquake of a single magnitude. An M_w 7 earthquake would have an average rupture length of 45 km and a displacement of about 1 meter (Wells and Coppersmith, 1994). At a slip rate of 10 mm/yr, it would take that section of fault 100 years without breaking to accumulate 1 meter of slip deficit. Earthquakes therefore should occur on average once every 100 years. This corresponds to an annual rate of 0.01 that an M_w 7 earthquake will occur on this section of fault in any given year. If, instead, the fault exhibits Gutenberg-Richter behavior, which means that the fault ruptures with an exponential distribution of magnitudes (for example, M_w 5 being 10 times more frequent than an M_w 6), then an annual probability can be assigned to each magnitude range such that when the displacements of all of the ruptures are summed over a given period of time, they yield the slip rate of the fault.

Earthquake Ground Motions

Once source locations and probabilities have been defined, we need to know the ground motions that those sources will produce as a function of period, magnitude, and distance from the source. The ground-motion relations, also referred to as attenuation relations, are generally defined in terms of peak ground acceleration and spectral acceleration at multiple periods. This is done because, depending on the size and stiffness of a structure, there will be a specific ground-motion period to which the structure is most sensitive.

These equations are found empirically when sufficient data are available or are derived theoretically otherwise. There is usually large variability in the ground motions for a given source at a specified distance. As a result, ground-motion relationships provide both the median ground motions and their variability. Because of this uncertainty in ground motions, we can say for example that at a given magnitude and distance, the probability of exceeding the median ground motion is 50 percent. The probability of exceeding twice the median ground motion will depend on the variability of ground motion. Most studies find a normal distribution of ground motions on a logarithmic scale such that the median plus one standard deviation is within a factor of two of the median. If, for a given magnitude and distance, the median ground motion is 50 percent *g*, one standard deviation above would be 100 percent *g*, and one standard deviation below would be 25 percent *g*. The probability of exceeding 25 percent *g* would be 84 percent, and the probability of exceeding 100 percent *g* would be 16 percent.

Earthquake Intensity and Damage

Once seismic hazard maps have been produced, users of the maps can go from seismic hazard to risk, relating ground motions to structural damage and loss. Engineers will typically

do this with the use of vulnerability curves. Given the way in which a structure is built, it will respond in a certain fashion to ground motion. Again, like the ground-motion relationships, vulnerability curves have considerable variability about their mean. For example, if an unreinforced masonry residence built without seismic requirements, the type of residence most common in northern Pakistan (Ali, 2005), experiences 50 percent *g*, which is approximately the 1-second spectral acceleration with a 2-percent probability of being exceeded in 50 years in Kabul, then there is a 50-percent chance that just over 18-percent damage to the home would occur. But because of the variability in vulnerability of structures, nearly 70 percent of these types of homes would experience between 4- and 30-percent damage. Many homes could be untouched and many could be destroyed. Closer to the seismic source, larger ground motions, and hence greater damage, would occur.

Another means of assessing damage is with the use of an intensity scale such as the Modified Mercalli Intensity (MMI) scale (Wood and Neumann, 1931; Richter, 1958) or European Macroseismic Scale 1998 (Grunthel and others, 1998). These scales relate ground motion and earthquake damage. Table A1 presents an intensity scale coupled to ground accelerations (Wald and others, 1999) such as those found on the seismic hazard maps, modified for construction practices in northern Pakistan (Ali, 2005), an acceptable analog for Afghanistan. If Kabul were subject to a large earthquake ground motion in which the peak ground acceleration were 50 percent *g*, the value for which there is a 2-percent probability of exceeding in 50 years, then, based on table A1, an intensity of VIII could be expected. People at such a location would experience severe shaking, their furniture overturned, and many unreinforced masonry buildings would suffer moderate to heavy structural damage. Note, however, that these intensity scales do not account for the secondary effects of ground motion, such as fires or landslides as occurred in the 1906 California earthquake and the 2002 deep Hindu Kush earthquake.

Table A1. Seismic Intensity scale with relation to ground motion.[1]

PEAK ACC.(%g)	*<.17*	*.17-1.4*	*1.4-3.9*	*3.9-9.2*	*9.2-18*	18-34	34-65	65-124	>124
PEAK VEL.(cm/s)	<0.1	0.1-1.1	1.1-3.4	3.4-8.1	*8.1-16*	*16-31*	*31-60*	*60-116*	*>116*
ESTIMATED INTENSITY	I	II-III	IV	V	VI	VII	VIII	IX	X+

	Descriptions
I	Not felt, no items displaced, and no damage.
II	Scarcely felt, no items displaced, and no damage.
III	Weak shaking, hanging objects swing slightly, and no damage.
IV	Mild shaking, hanging objects swing and windows and doors rattle, and no damage.
V	Moderate shaking, hanging objects swing considerably and precarious objects may fall over, and negligible damage to unreinforced masonry buildings.
VI	Strong shaking with few people losing their balance, furniture may be shifted, and few unreinforced masonry buildings suffer slight structural damage.
VII	Very strong shaking and difficult to stand, objects fall from shelves, and many unreinforced masonry buildings will suffer slight to moderate structural damage and few will experience moderate to heavy structural damage.
VIII	Severe shaking, furniture overturned, and many unreinforced masonry buildings will suffer moderate to heavy structural damage and few will experience heavy to very heavy structural damage.
IX	Violent shaking with people forcibly thrown to the ground, monuments and columns fall, and most unreinforced masonry buildings will suffer heavy to very heavy structural damage.
X+	Extreme shaking, and most unreinforced masonry buildings will suffer very heavy structural damage.

[1] Table derived from Grunthel and others (1998) and Wald and others (1999) and is based on a structural vulnerability class of A and B, which corresponds to unreinforced brick masonry, simple and rubble stone, and adobe construction.